Kaltenegger Martin, BSc

Polymorph selection in nabumetone thin films at surfaces

MASTER'S THESIS

to achieve the university degree of

Master of Science

Master's degree programme: Advanced Materials Science

submitted to

Graz University of Technology

Supervisor

Ao. Univ.-Prof. Dipl-Ing. Dr.techn. Roland Resel

Institute of Solid State Physics

Graz University of Technology

Graz, April 2018

Affidavit

I declare that I have authored this thesis independently, that I have not used other than the declared sources/resources, and that I have explicitly indicated all material which has been quoted either literally or by content from the sources used. The text document uploaded to TUGRAZonline is identical to the present master‘s thesis.

Date	Signature

Acknowledgement

I would first like to thank my thesis advisor Professor Roland Resel of Institute of Solid State Physics at the Graz University of Technology for supervising me through my master thesis.

Furthermore, I would like to thank my co-supervisor Dr. Oliver Werzer for his support. Oliver's office was always open whenever I had questions or some troubles about my research or writing. He consistently allowed this thesis to be my own work, but steered me in the right direction whenever he thought I needed it.

I would also like to thank the experts from the Elettra Synchrotron Trieste for their support during my measurements there: Luisa Barba and Nikola Demitri. Without their passionate participation and input, the validation survey could not have been successfully conducted.

I am deeply grateful for the wonderful collaboration given by Christian Röthel and Benedikt Schrode. Special thanks should be given to Stefan Pachmajer, Paul Christian and Sebastian Hofer for their willingness to help me always I had a question. I would also like to extend my thanks to the iCVD group of Professor Anna Coclite. Special thanks to the memebers of the team of the Solid State physics and the team Pharmaceutical Technology from the Graz university.

Finally, I wish to express my very profound gratitude to my parents, to my family and all my friends for providing me with unfailing support and continuous encouragement throughout my years of study and through the process of researching and writing this thesis. This work would not have been possible without them. Thank you.

Abstract

The investigation of polymorphic structures is important for different scientific fields, like pharmaceutical technologies and organic electronics. Controlled conditions for crystal growth are important, since polymorphs have a strong influence on different properties like thermodynamic and chemical stability, and important for pharmaceutics, the bioavailability. Nabumetone is a non-steroidal anti-inflammatory drug, which forms two polymorphic phases. Where form 1 is the more stable phase and form 2 the less stable phase. The idea of this work is to study the polymorphism within thin films. For that case different deposition methods like spin coating, drop casting and dip coating were employed. Nabumetone was dissolved in different solvents like ethanol, toluene and tetrahydrofuran. Furthermore, polymer chains were added to the solutions. The crystallographic phase analysis was obtained by X-ray diffraction experiments. It transpired that the use of deposition method where slow evaporation rates, like drop casting and dip coating, are applied, due to the Ostwald rule of stages, nabumetone crystallized in form 1, with a 204 texture, meaning the molecules are lying on the substrate. Furthermore, form 1 crystals occurred mostly in needle like structures but also in small plates. A change in the evaporation rate of the solvents, applying spin coating, results for high concentrated solution again in polymorph 1, regardless of whether fast or slow spin velocities were used. At lower nabumetone concentration dewetting started to appear and resulted in the formation of form 2 crystals, which build small islands on the substrates. The X-ray diffraction experiments revealed standing molecules of form 2, which recrystallized to form 1 over time with lying molecules. Moreover, additional peaks were found in X-ray diffraction experiments pattern. Which are assigned to a new polymorphic form. Additionally, applying polymer matrices nabumetone molecule formed amorphous solid-solid conformations in the matrices, whereas residual molecules crystallized in both polymorphic phases. In general, the production of nabumetone thin films showed that the formation of the stable phase 1 predominates, whereas the less stable form 2 and the new form appeared only in spin coating processes at low initial nabumetone concentrations. Which reveals that form 2 and the unknown form needs the sample surface to crystallize. However, the surface does not stabilize these two forms.

Kurzfassung

Die Untersuchung der polymorphen Strukturen ist ein wichtiger Gegenstand in unterschiedlichen wissenschaftlichen Bereichen, wie zum Beispiel in den pharmazeutischen Technologien und in der organischen Elektronik. Kontrollierte Bedingungen während des Kristallwachstums sind wichtig, da polymorphe Phasen einen starken Einfluss auf verschiedene Eigenschaften wie die thermodynamischen und chemischen Stabilität und die Bioverfügbarkeit haben. Nabumeton, ein nichtsteroidaler Entzündungshemmer, besitzt zwei polymorphe Phasen. Form 1 ist hierbei die stabile und Form 2 die instabilere Phase. Die Idee dieser Arbeit ist es, diesen Polymorphismus in dünnen Filmen zu untersuchen, weshalb verschiedene Beschichtungsmethoden wie Spin-Coating, Drop-Casting und Dip-Coating eingesetzt wurden. Nabumeton wurde in verschiedenen Lösungsmitteln wie Ethanol, Toluol und Tetrahydrofuran gelöst. Zusätzlich wurden auch Polymere zu den Lösungen hinzugefügt. Für die kristallographische Phasenanalyse wurden verschiedene Röntgenbeugungsexperimente durchgeführt. Diese zeigten, dass die Anwendung von Depositionsmethoden mit einer langsamen Verdampfungsrate, wie es bei Drop-Casting und Dip-Coating der Fall ist, und aufgrund der Ostwaldschen Stufenregel, vorwiegend Polymorph 1 kristallisiert mit einer 204 Textur, was bedeutet, dass die Moleküle flach auf dem Substrat liegen. Die Kristalle der Form 1 traten in nadelartigen Strukturen und auch in kleinen Plättchen auf. Auch eine Änderung der Verdampfungsrate der Lösungsmittel durch Spin-Coating bei hochkonzentrierten Lösungen führte zur Kristallisation in Form 1, unabhängig von den Spin-Geschwindigkeiten welche angewandt wurden. Bei niedrigeren Nabumeton-Konzentrationen entstanden Entnetzungsflächen, welche zur Bildung von Form 2 führten, die auf den Substraten die Form von kleinen Inseln besaßen. Röntgenbeugungsexperimente zeigten, dass Form 2 aus stehenden Molekülen bestand, die sich im Laufe der Zeit zu Form 1 umkristallisierten. Darüber hinaus wurden zusätzliche Peaks in den Röntgenbeugungsexperimenten gefunden,welche einer neuen polymorphen Form zugeordnet werden. Zusätzlich kam es durch die Verwendung von Polymermatrizen zu einer amorphen Solid-Solid-Konformation, wobei überschüssige Moleküle auf der Polymeroberfläche in beiden polymorphen Phasen kristallisierten. Im Allgemeinen zeigte die Herstellung von Nabumeton Dünnfilmen, dass die Bildung der stabilen Form 1 überwiegt, während die instabilere Form 2 und eine neue Form durch Spin-Coating bei niedrigen Nabumeton Konzentrationen hergestellt werden konnte. Diese Ergebnisse zeigten, dass die Form 2 und die unbekannte Form eine Oberfläche benötigen um zu kristallisieren, wobei diese Oberfläche diese zwei Formen nicht stabilisiert.

Contents

Chapter 1

Introduction

The understanding of crystallization processes is a crucial theme in material science.[1] Since, controlling the crystallization can be used to achieve various material properties, for instance the chemical stability, thermal responds, dissolution properties a. o. For many application bulk crystallization is helpful, but the access to different polymorphic structures is limited. Polymorphism describes the behaviour of a solid to exist in different crystal structure while keeping its chemical structure identical.[2] To get an access to these structures, heterogenous nucleation is applied as a tool for polymorph selection.[3] Since some phases are only achieved by employing surfaces, thin films technologies occur as a terrific opportunity. Furthermore, these methods allow the variation of thermodynamics and kinetics during the crystallization process. From a pharmaceutical point of view the application of such thin film layers in plasters and implants is an alternative to conventional therapies, by taking tablets. In principle, more unstable phases allow a faster dissolution, which results in a better bio-availability.[4] Thus, a detailed knowledge of the polymorph selection in thin films are required.

1.1 Nucleation theory

Due to its importance the formation of crystals, polymorph selection, has been under investigation since decades and the first step of crystallization is the nucleation process.[5] It is a process, which plays a big role scientfic technology. Moreover, it is present in many natural phenomena like snow or the vesication during phase transitions.[6] Nucleation is not only the first step but it seems it is also the main step which determines the type of polymorph phase. Thus many experimental techniques and computational simulations were applied to get detailed information of the nucleation step.[7] Until now two different hypotheses were established. The

simpler one is the Classical Nucleation Theory (CNT), where the nuclei form clusters already with the same structure like the mature crystal. The second theory describes a non-classical nucleation pathway. Here, the nucleation process happens in two steps.[3] Both types are shortly summarized in the following.

1.1.1 Classical Nucleation theory

The CNT introduced by Volmer and Weber and enhanced over the years, predicts basically the formation of a liquid from the vapour phase. This knowledge can also be used to describe crystallization from solution or melt. Atoms /molecules in a solution can be due to fluctuation attached to other atoms and form a nucleus. The probability to form a nucleus is described by following equation:[7]

$$I_{nuc} = I_0 exp(-\frac{\Delta G*}{k_B T}) \tag{1.1}$$

Here, I_0 is a kinetic prefactor which consist of the number of nucleation sites and the probability of a nucleus not to dissolve. k_B is the Boltzmann constant and T the temperature. The nucleus can now collapse or grow and build a crystal. That behaviour is described thermodynamically by the free energy barrier ΔG*, which have to be overcome therewith the nucleus stays stable. Generally, two different mechanism of nucleation exists. The first is the homogeneous nucleation, where the nucleation happens due to supersaturation in the liquid phase.[8] Heterogeneous nucleation on the other side happens due to dust or on surfaces.[9] Homogeneous nucleation is found more rarely than the heterogeneous nucleation, but is easier to describe. Due to supersaturation in the solution sufficient atoms/molecules are present to form a nucleus. The energy barrier ΔG* consists of two different term, which depends on the radius of the spherical nucleus.[6]

$$\Delta G^* = \Delta G_V + \Delta G_S = \frac{-4\pi r^3}{3v} k_B T \ln S + 4\pi r^2 \sigma \tag{1.2}$$

The first term represents the volume part of the nucleus. It is the free energy win which one gets for the growth in volume and increases with r^3. Here, v is the volume of a single molecule and S is the supersaturation ratio. The second term derives from the energy, which is needed to increase the surface area. The energy increases here with r^2. Thus, it can be seen that for small r the surface term dominates. By increasing the radius, the volume term starts to increase more quickly. Consequently, the total free energy at first increases and after reaching a maximum value it will decrease.[5] In Figure 1.1 this behaviour is graphical represented.

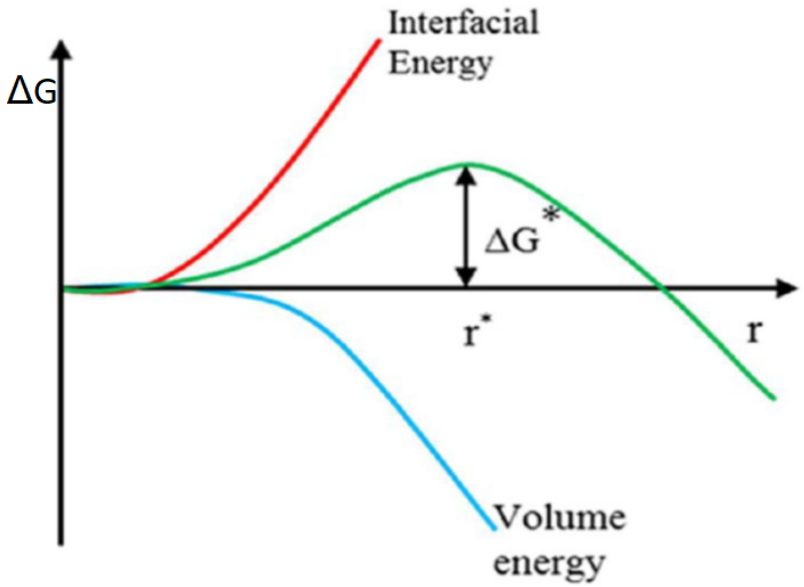

Figure 1.1: Contribution for the formation of the nucleation barrier ΔG^* in dependence on the radius r.[6]

As already mentioned the maximal free energy ΔG* determines an energy barrier which the nucleation has to overcome for stabilization. From that barrier the critical nucleus radius r* can be determined from which the nucleus exists in an equilibrium state; it can dissolve or growth. When the nucleus is bigger than r* it stays stable and will growth to form a crystal.
In the case of heterogeneous nucleation, the nucleation starts at surfaces.[10] Here, through the surface it cannot assumed that the nucleus is a sphere. Therefore, the surface term of Equation 1.2 has to be modified by terms of surfaces tensions and some other factors.[9] In Figure 1.2 the influences on the surface terms are depicted.

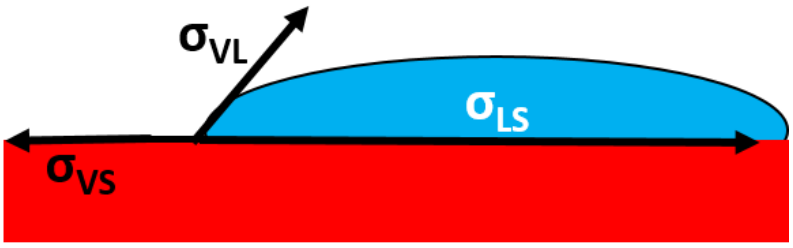

Figure 1.2: Schematic description of the heterogeneous nucleation dependence on different tension terms: σ_{LS} the tension between liquid and solid phase, σ_{VL} tension between vapour and liquid phase, σ_{VS} tension between vapour and solid phase.

Consequently, the energy barrier ΔG* decreases and thus a lower level of saturation is needed for the formation of a stable nucleus. Nevertheless, the critical radius r* is

the same, regardless of whether homogeneous or heterogeneous nucleation take place. In general, heterogeneous nucleation occurs more often because a surface, especially in thin films, is available in most systems.[11],[12] Furthermore, when heterogeneous nucleation appears homogeneous nucleation is disfavoured.[10]

1.1.2 Non classical nucleation theory

The second prominent theory is the non-classical or two steps nucleation theory. This theory was introduced because new experimental techniques and simulations revealed that intermediate stages are present before a crystal or thermodynamically stable phase could be reached. At the two step nucleation only a low level of saturation is required. However, fluctuation of the density in liquid state leads to phase separation of a dense liquid phase, liquid like clusters without a preferred orientation and an 'empty' liquid phase. The nucleation starts in the second steps in these liquid clusters. The nucleation mechanism itself stays the same for both the CNT and the non-classical nucleation theory.[13],[3]

1.2 Crystallography

Due to the easier processibility and better storage possibilities crystallinity is very important for different fields in science like photovoltaics and pharmaceutics. Moreover, the stability seems often to be better if the material is present in a solid state. In principle, molecules can exist in different solid state forms. For instance if the molecules have no arranged periodical defined order the molecules are amorphous solid. However, the molecules can arrange with a long range order, where the molecules assemble in a defined periodical lattice.[14] For reasons of stability mainly two different non covalent bond types exist between the molecules. The first one are Van der Waals bonds. Here, the bond is formed by weak dipole-dipole interactions between the molecules. Additional to those bond hydrogen bonds frequently appear in molecular crystals. Hydrogen bonds are described by the bond of a hydrogen atom to a high electronegative charged atom like oxygen or nitrogen.[15]
As a consequence of these intermolecular bonds, long range ordered molecules or atoms build a lattice. This lattice is described mathematical by sequenced equivalent lattice points. Starting with one point all other points can be reached by the translation vector. Every translation vector $\mathbf{T}$ consists of three different vectors, the lattice vectors: $\mathbf{a}$, $\mathbf{b}$, $\mathbf{c}$.[16]

$$\mathbf{T} = n_1\mathbf{a} + n_2\mathbf{b} + n_3\mathbf{c} \tag{1.3}$$

n_1, n_2, n_3 are integers. To get a real physical crystal structure every lattice point must be occupied by a basis which consists of atoms or molecules. The lattice vectors **a**, **b**, **c** generates the unit cell which is the repeating unit of a crystal structure. This unit cell is primitive, when none other cell with a lower volume exists from which the crystal structure is formed. Beside the translation, different symmetries exist. Consequently, every lattice point can be transformed into every other one. In principle one can distinguish between three simple sorts of symmetry; rotation, inversion and reflection. Thus, through the translation vectors and the three symmetries 14 different Bravais lattices are defined. Those Bravias lattices can be divided into 7 lattice systems; triclinic, monoclinic, orthorhombic, tetragonal, hexagonal and cubic. In Table 1.1 the crystal systems with their different lattices are depicted. The lattice parameters a, b, c are the side length and α, β, γ the corresponding angles between the unit cell vectors.[16]

Table 1.1: Lattice constant and angles of the different crystal systems[15]

Crystal system	Lattice axes	Axes angles
triclinic	a $\neq$ b $\neq$ c	$\alpha \neq \beta \neq \gamma$
monoclinic	a $\neq$ b $\neq$ c	$\alpha = \gamma = 90° \neq \beta$
orthorombic	a $\neq$ b $\neq$ c	$\alpha = \beta = \gamma$
tetragonal	a =b $\neq$ c	$\alpha = \beta = \gamma = 90°$
rhombohedral	a =b = c	$90° \neq \alpha = \beta = \gamma < 120°$
hexagonal	a =b $\neq$ c	$\alpha = \beta = 90°; \gamma = 120°$
cubic	a = b = c	$\alpha = \beta = \gamma = 90°$

1.2.1 Polymorphism

The behaviour of a crystal to exist in different crystal packing is called polymorphism.[2] Due to the wide spread where polymorphism can be found the investigation on it is an important field in material science. Especially for semiconductor science and pharmaceutics it is important to understand the polymorph selection.[17],[1]
In pharmaceutics polymorphism is essential for medication. For instance, a controlled and reproducible drug formulation is required to guarantee same therapeutic action on every treatment.[18],[19] Moreover, changes in polymorphism changes the properties from which new and superior drug formulation can be obtained. Metastable or amorphous phase allow faster dissolution in the stomach or the blood and as a consequence a better bio-availability and a lower risk of side effect can be reached. Thus, regularity approval is required for each polymorphic phase individually.[20]

In principle, polymorphic materials always have one bulk phase, which is due to the lowest enthalpy the most stable one.[21] Whereas, thin film phases are regularly the metastable form.[22] Due to distinct stabilities, spontaneous recrystallization from a metastable phase to the bulk phase can happen. Such transitions between two polymorphisms can be monotropic. The transitions below the melting point from one phase to another form, in many cases from the metastable phase to the bulk phase is irreversible.[2] The following table reveals some examples of pharmaceutical molecules which possess two or more polymorphic phases.

Table 1.2: Examples of pharmaceutical molecules and their number of polymorphic phases.[23],[24],[25],[4],[26],[27]

pharmaceutical agent	polymorphic phases
Paracetamol	2 bulk phase, 1 metastable phase
Caffeine	2 bulk phase
Phenytoin	1 bulk phase, 1 thin film phase
Carbamazepine	5 bulk phases
Aspirin	2 phases

1.3 X-ray diffraction

X-ray applications are used in many different fields, e.g. in medicine to investigate health issues, in material testing and many others. X-ray radiation is an electromagnetic radiation, which can occur through two different fundamental processes. The first origins due to a strong acceleration of electrons by hitting matter or bended in a electromagnetic field and is named bremsstrahlung. The second origins from an electron which has enough energy and hits an atom and can knock out a electron from an inner atomic shell. The produced vacancy fills up with an electron from a higher energy level. Differences in both energies is emitted as characteristic X-rays.[28] The emission spectrum varies for every material. Thus, the X-ray wavelength varies between 0.01-10 nm and possess energies in the range of 10 eV to 100 KeV. The wavelength λ can be transformed into the energy E via:

$$\lambda = \frac{c}{f} = \frac{hc}{E} \tag{1.4}$$

h represents the Plank constant, c is the speed of light in the used medium and f is the frequency. A special application, where X-ray radiation is a powerful technique to determine crystal structures is X-ray diffraction. With this technique many properties of a solid can be determined: the types and length of bond between

atoms and molecular packing informations which is required to understand physical properties.[29]

1.3.1 Bragg Law

The Bragg law is a condition for constructive interference and thus high diffracted intensity being observable in the experiment. A geometrical derivation of Bragg's law is illustrated in Figure 1.3.

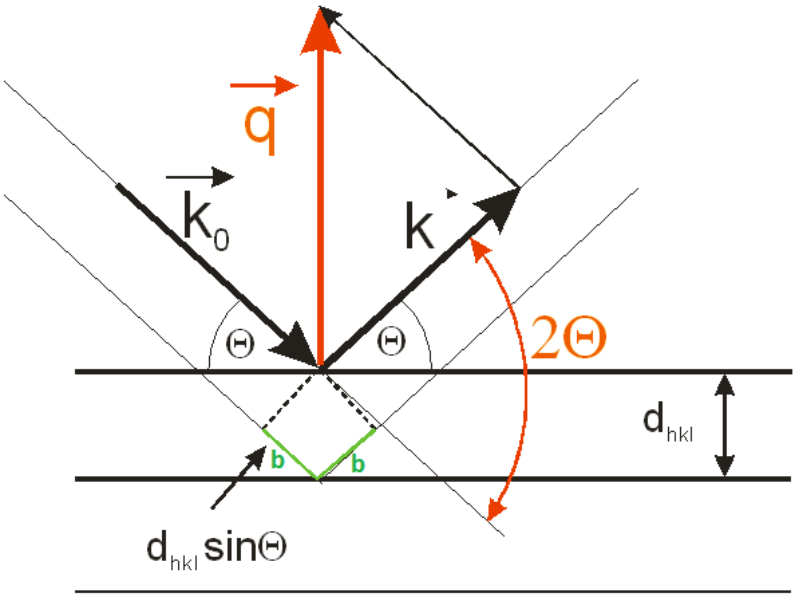

Figure 1.3: Geometrical derivation of the Bragg law and the Laue condition.[28]

It is shown that X-rays of a wavelength λ fall under an angle Θ onto a periodic structure formed by net-planes. One part of the wave is reflected on one plane under the same angle as the incoming angle. The second one is reflected on a plane separated with a distance d deeper lying plane also under Θ. The path differences of the reflected waves of the first plane and the second plane is 2b. Constructive interference can now only be observed when the path differences are an integer multiple of the incoming wavelength. Thus, the Bragg law can be written as:

$$n\lambda = 2b = 2d_{hkl}sin(\frac{2 * \Theta}{2}) \tag{1.5}$$

With d_{hkl} being the interplanar distance. The angle 2Θ describes the scattering angle.

1.3.2 Laue condition

Another approach to describe diffraction on a crystal is the Laue condition. In principle, both the Laue condition and the Bragg law are equivalent. However, the Laue condition describes the diffraction process in the reciprocal space. The real lattice can be very easily transformed into a reciprocal lattice via Equation 1.6.

$$\boldsymbol{b_1} = 2\pi \frac{\boldsymbol{a_2} \times \boldsymbol{a_3}}{\boldsymbol{a_1} \cdot \boldsymbol{a_2} \times \boldsymbol{a_3}} \qquad \boldsymbol{b_2} = 2\pi \frac{\boldsymbol{a_3} \times \boldsymbol{a_1}}{\boldsymbol{a_1} \cdot \boldsymbol{a_2} \times \boldsymbol{a_3}} \qquad \boldsymbol{b_3} = 2\pi \frac{\boldsymbol{a_1} \times \boldsymbol{a_2}}{\boldsymbol{a_1} \cdot \boldsymbol{a_2} \times \boldsymbol{a_3}} \tag{1.6}$$

With a_1, a_2, a_3, the lattice vectors and b_1, b_2, b_3 are the primitive reciprocal lattice vectors. From these vectors a reciprocal lattice vector is defined by:

$$\boldsymbol{G} = h\boldsymbol{b_1} + k\boldsymbol{b_2} + l\boldsymbol{b_3} \tag{1.7}$$

With hkl integer numbers. **G** defines now the possible reflection through diffraction. For the derivation one has to consider the scattering of an incoming wave vector $\boldsymbol{k_0}$ on a sample into the direction of the scattered vector **k**. [29]
The change of the wave vector, mathematical the difference of the incoming and the outgoing vector **k** - $\boldsymbol{k_0}$, is named the scattering vector **q**. Constructive interference can be only observed when **q** is parallel to the net plane normal n_{hkl} or in other words the incoming angle is the same as the reflected angle. Thus, the Laue condition is defined as:[15]

$$\vec{\boldsymbol{q}} = \vec{\boldsymbol{G}} \tag{1.8}$$

Chapter 2

Experimental techniques

In this thesis samples were prepared by different solution deposition techniques. Therefore, the used drug had to be dissolved in various volatile solvents, which will be discussed below. The prepared samples were investigated by light microscope respectively by polarized light microscopy and by X-ray diffraction techniques (specular scanning and grazing incidence X-ray diffraction).

2.1 Sample preparation

For the sample preparation various techniques had been employed. In principle surfaces are coated with a solution containing the molecule. After solvent removal a film formed by the drug molecule remain on the surface. In general there are many techniques possible for such preparation with each providing different parameters for the crystallization process.[30] Within this work, this should provide some possibilities for polymorph selection. In Figure 2.1 various methods are schemed and in the following the most relevant for this work are explained in more detail.

2.1.1 Drop casting

Drop casting is a easy methods for depositing a film on a substrate. There, the solution is dropped on the surface. After some time the solvent evaporates and the retarded material forms crystallits at the surface. The film thickness can in principle varied by the used concentration and the amount of deposited solution. Nevertheless, some additional effects can influence the film formation. Firstly, it depends on how the solution wets the surfaces and on capillary forces with the surface during drying. Secondly the evaporation rate of the solvent affects the crystallisation process. By

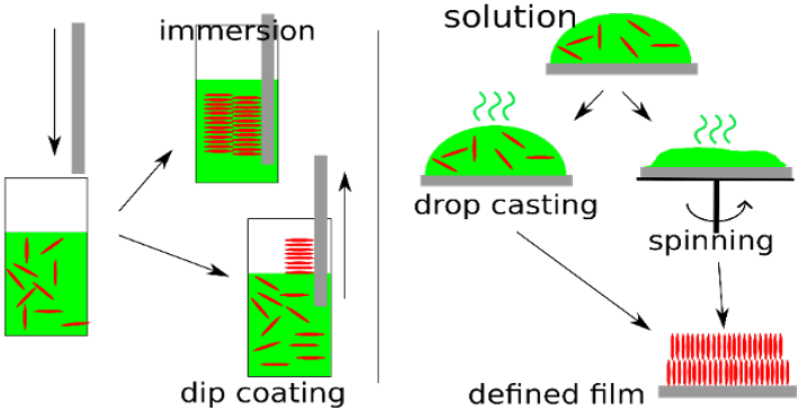

Figure 2.1: Overview about the used chemical solution deposition methods: drop casting, spin coating, dip coating

covering the samples with a petri dish a solvent depended atmosphere is created, which decreases the evaporation rate. The tighter the cover the slower the evaporation rate will be and as a consequence molecules get more time for crystallisation. On these grounds, drop casting is closer to thermodynamic equilibrium.[31]

2.1.2 Spin coating

Spin coating is a widely used preparation method, applied for instance by industries to produce thin films for micro-electrical device prepeats. After the deposition of the solution, the substrate rotates. Since, the centrifugal force forces the solution to spread over the substrate the whole surface is wetted. During the rotation already some of the solvent evaporates, ejected across the edge of the surface and in a subsequet step the sample can be dried by continuous spinning. For sample preparation here the used substrates were rotated until they were completely dry. With this method homogeneous thin films were obtained. By changing some of the parameters changes in the resulted film can be induced. For instance, by varying the solution concentrations the viscosity is changed and as a consequence thicker films care prepared. This also changes the crystallisation process. Another advantage of spin coating is the possibility to set the spin velocity. In principle, faster spinning results in thinner films. Moreover, the evaporation rate is increased and thus other crystal formations can appear. The biggest disadvantage of the spin coating method occur at relative high spin velocities. Here, a lot of material is washed away from the substrate and gets lost. Nevertheless, spin coating is one of the most powerful method for thin film preparation and was extensively used in this thesis.[32],[33],[34]

2.1.3 Dip coating

The third deposition technique used for sample preparation, was dip coating. With this method the substrates are immersed into a solution. After a short hold time, the withdrawal process, the most important sub-process starts. Here, it is essential for the film formation how fast this process proceeds, because at the interface between solution and vapour the film growths. Various effects can influences the growth. On one hand solution can flow back into the container, which means when withdrawl process is too fast more solution will stay back on the substrate; thicker film on substrates is resulted. On the other hand capillary forces affects an upwards solution flow for a few mm, which typically depends on the interaction between solvent/solution and the used substrates. Especially at the beginning of the withdrawl process and at the liquid-vapour interface that behaviour influence the film growth most, whereas the back-flow is more dominant at later stages. However, in principle a slower withdraw speed resulted often in thinner films.[35],[34]

2.2 Polarized light microscopy

Polarized light microscopy is an optical investigation technique to investigate, morphological of thin films. This technique is powerful and also a quick process. A polarized light microscope posses two polarisation filters, the polariser and the analyser. When light hits the polariser, only waves of a specific orientation of the e-field can pass the filter. The light is then polarized. The analyser is aligned perpendicular to the the first polarizer. Due to, optical properties of a crystalline solid the polarization direction can be rotated and as a consequence some light passes the analyser and a bright picture of the solid is observed. A solid, which shows the described properties are called optical anisotropic or birefringent. This behaviour can be further used to determine the crystal thickness of the observed crystal via the Michel-Levy birefringence chart.[36] For the investigations in this thesis microscopes from Olympus (BX51) and Zeiss (Zeiss AxioVert) were used.

2.3 Specular XRD

Specular X-ray diffraction is used to measure crystalline properties of samples.[37],[38] By using a defined incident angle of Θ and a symmetric exit angle Θ the scattering angle results to 2Θ. Constructing the scattering vector $\mathbf{q}$ from this two angles shows that the vector remains always perpendicular to the sample surface (Figure 2.2)[39]. As a result only net-planes which are parallel to the surface can be detected by such

a measurement.

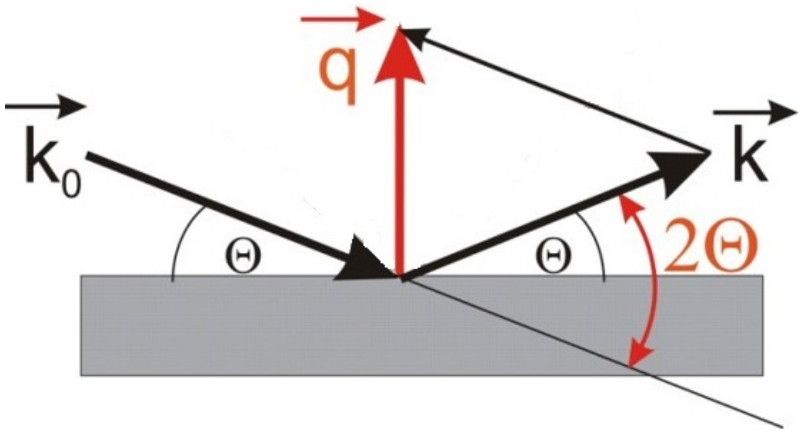

Figure 2.2: Scheme representing the specular X-ray diffraction

The geometry of the used Θ/Θ diffractometer, a PANalytical Empyrean is depicted in Figure 2.3. Beginning with the copper X-ray tube $\lambda = 0.154$ nm, which operates at 40 mA and 40 kV, a primary beam optic is attached, with a 1/8°divergence slit and a 10 mm beam mask. Furthermore, a parallel beam mirror is applied to transform the divergent X-beam beam into a more parallel one. To ensure that the beam intensity is not too high to destroy some detector elements a beam attenuator is used. This attenuator consists of a Ni-plate, which is inserted into the beam when the intensities at the detector reach a set value. Due to, the sample stage the investigated samples can be rotated, lifted and tilted. At diffracted beam path, which is basically observed at a 2Θ angle, a anti-scatter slit with a height of 7.5 mm is built-in. This anti-scatter slit reduces the background signal. For reducing the peak asymmetry due to axial divergency a 0.02 rad. Soller slit is implemented in the measurement set-up. The PIXcel3D 1x1 detector is a solid state area detector and operated in 1D scanning mode with 255 active channels. The adjustment of the incident and the diffracted beam is controlled by a goniometer.

2.4 Grazing incidence X-ray diffraction

The Grazing Incidence X-ray Diffraction (GIXD) is a X-ray technique to get crystallographic in-plane information from thin films[40], i.e. from directions which are not parallel to the surface.[41] Here, the angle of incidence α_i is typically small, in the range of the critical angle α_c. Moreover, α_i is different form the half of the diffracted

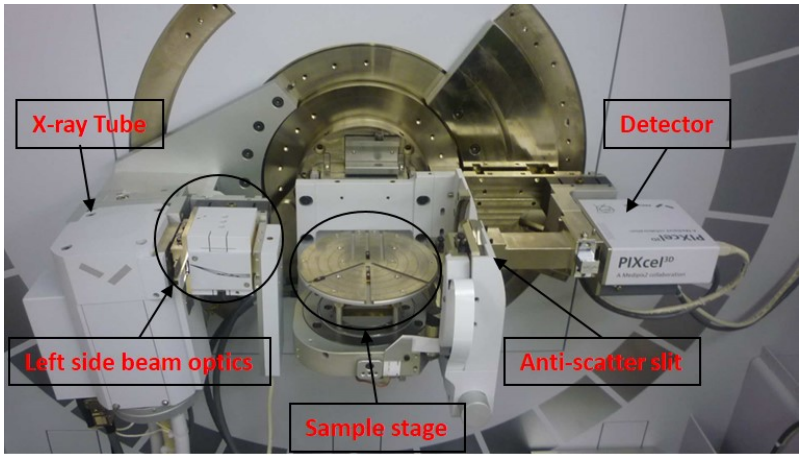

Figure 2.3: The measurement set-up of the PANalytical Empyrean, in the background the goniometer can be observed

beam 2Θ.[42] When X-ray beam hits the sample at such small angles an evanescent wavefield is formed. This wavefield runs parallel to the surface and can be used to do diffraction on periodic structures, with net-planes, which are not parallel to the surface area. By increasing α_i the penetration depth can be increased.[29] Figure 2.4 represents the GIXD geometry.

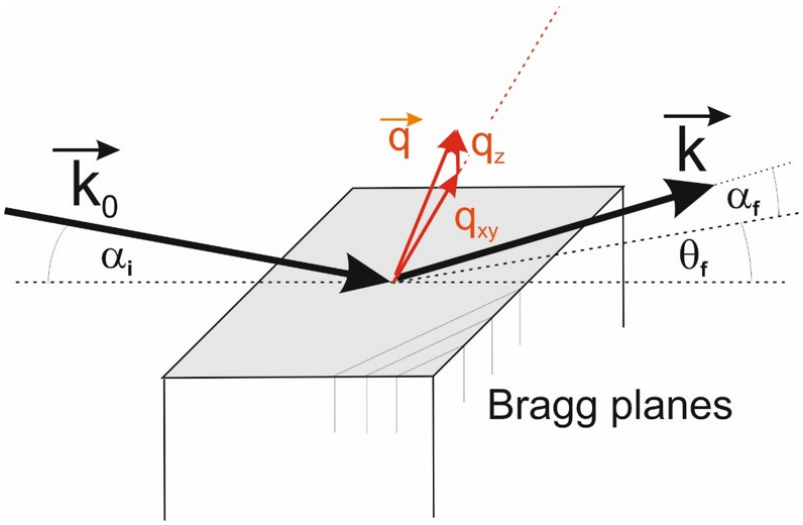

Figure 2.4: Schematic geometry in GIXD, the incidence angle is constant during the investigation

GIXD measurements were done on the Elettra synchrotron Trieste XRD 1 beamline. Here data are collected by a large 2D Dectris Pilatus 2M detector with about 2 million pixels. Meaning large areas of the reciprocal space can be measured. A high energetic X-ray beam with a wavelength $\lambda = 0.14$ nm ($E = 8.86$ KeV), was used which provided by a bending magnet. This method also provides much more photon

intensity with which one can measure much faster compared to the lab. Additionally rotating the samples by 360°many reflections can be observed as an ideal 2D-powder is generated. The results from the measurement are transformed into a reciprocal space map. In the reciprocal space map q_{xy}, x-axes, describes the in-plane ratio and q_z is the of the out-of-plane ratio from the diffracted beam. From the reciprocal space maps crystal structures and orientation (texture) of thin film crystals can be solved.[29]

Chapter 3

Material for sample preparation

In this chapter the used pharmaceutical molecule nabumetone beside the different solvents (ethanol, toluene, tetrahydrofuran) and polymer matrices (polystyrene, poly(mathyl methacrylate)) used for sample preparation are introduced.

3.1 Nabumetone

Nabumetone (4-(6-Methoxy-2-naphthyl)butan-2-on) is an anti-inflammatory drug. This molecule was launched in 1985 and is used for the treatment against swelling, pain and stiffness from arthritis.[43] Thus, nabumetone shows some similarities with the pharmaceutical drug diclofenac, which is the main ingredient in Voltaren.[44] Nabumetone is mainly ingested oral. Afterwards it is transformed by the human organ liver to 6-Methoxy-2naphthylacetic acid, which then has the biological relevant performance. Therefore nabumetone belongs to the class of pro-drugs. Benefits of the drug are on one side the low toxicity even at high doses and on the other side the lower risk of side effects compared to other anti-inflammatory drugs. The nabumetone molecule consists of a 2-naphthyl rest in the middle, a head group (methoxy group) and a tail group (butanone rest). In Figure 3.1 the structural formula of the nabumetone molecule is depicted.[43]

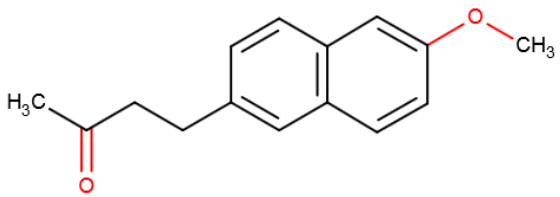

Figure 3.1: Structural formula of the nabumetone drug

In literature the polymorphism of nabumetone is discussed to have two polymorphic phases. Polymorph 1 is described as the bulk phase of nabumetone, thus the thermodynamically more stable phase. This polymorph forms a monoclinic system with eight molecules in the unit cell.[45] The corresponding lattice constants are shown in Table 3.1. The molecules in the unit posses a head to tail arrangement (Figure 3.2a), which stabilizes this phase by C–H$\cdots$O contacts. Form 1 has a melting point T_m at about 80°C and a material density $\rho = 1.26\ \frac{g}{cm^3}$.[46]

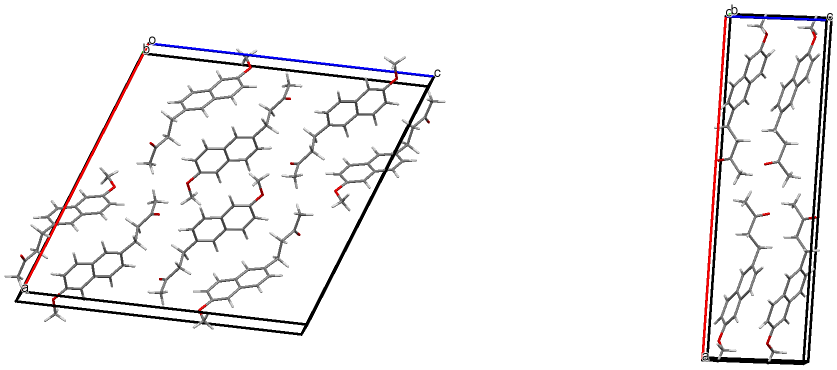

(a) (b)

Figure 3.2: Unit cells of nabumetone polymorphs a): polymorph 1, b): polymorph 2

Table 3.1: Lattice constants of the two nabumetone polymorph phases[46]

	Form 1	Form 2
a ($\mathring{A}$)	21.8603	26.9485
b ($\mathring{A}$)	5.3335	5.8773
c ($\mathring{A}$)	22.2337	7.8960
α (°)	90	90
β (°)	111.9288	91.767
γ (°)	90	90
V ($\mathring{A}^3$)	2404.71	1250.0

The second phase of nabumetone, polymoprh 2, is thermodynamically less stable. It crystallizes also in monclinic crystal system, but only posses four molecules in its unit cell. The corresponding lattice constant are shown in Table 3.1. In contrast to form 1, the molecules here pack in a tail to tail group arrangement. The space group for both polymorphs are in the $P2_1/c$ group. Thermal investigations showed that the melting temperature lies below of this of form 1 at 65°C. The material density is decreased ($\rho = 1.21\ \frac{g}{cm^3}$).[45] Due to the different C–H$\cdots$O inter-molecular contacts(short contacts) the molecules of polymorph 1 forms infinite sheets, which stabilize this polymorphic form. Those contacts for polymorph 2 are weaker and

as a consequent this form is less stable.[46] The following figure Figure 3.3 reveals the calculated powder pattern of both nabumetone forms and the differences in the conformation of the nabumetone molecules in the both unit cells. It can be seen that the conformations showed only small differences due to single bonds.

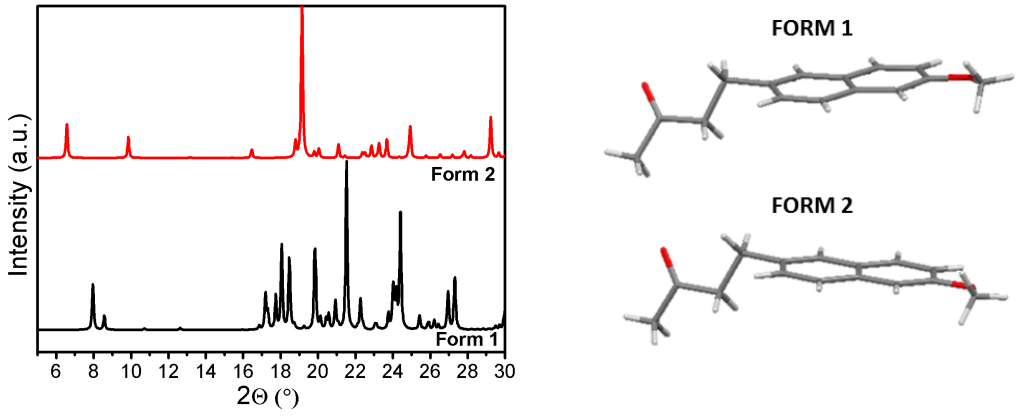

(a) (b)

Figure 3.3: a): Calculated powder pattern and b): differences in the conformations of both nabumetone forms.

The solution preparation was done with a nabumetone-analytical standard (N6142) from SIGMA-ALDRICH. TLC measurements revealed a purity of 99%.

3.2 Solvents

3.2.1 Ethanol

Ethanol(C_2H_6O) is a solvent, which is used in many fields of our life. Furthermore, it is used in pharmaceutics and chemical industries as a solvent. The value of the boiling point is 78.24°C. At room temperature ethanol is colourless and easily inflammable. It posses a pungent odour. Due to the hydroxy group, ethanol has a hydrophilic behaviour, which allow the mixture with solvents of similar polarity, like water or chloroform. For solution preparation highly pure (96%) ethanol was used.[47],[48]

3.2.2 Toluene

Toluene(C_7H_8) is a colourless, very volatile solvent with a specific odour. Since, toluene posses similar solution properties as benzene, a poisonous solvent, it replaced benzene in many experiments. The value of the boiling point is for toluene 111°C. Water is not mixable with toluene, since toluene is nonpolar.[47],[48]

3.2.3 Tetrahydrofuran

The third solvent, which was used, is the organic solvent tetrahydrofuran (THF). THF($(CH_2)_4O$) belongs to the substance class of ethers and is at room temperature colourless and flammable. The boiling point amounts to 66°C. Moreover, it posses the characteristic smell of ether substances. By long contact with air and insolation THF can form through oxidation a peroxide, which can be easily explode. As a polar solvent THF is basically used for PVC, polystyrene, Poly(mathyl methacrylate), for paint and varnish.[47],[48]

3.3 Polymers

Polymers were used for two reasons. The first reason are their capabilities to work as a crystallisation inhibitor. Thus, the stabilities of amorphous states of the drug can be increased.[49] By using polymers matrices the mobility of the provided molecules are decreased and therefore the molecules needs a longer time for a specific arrangement. The second reason is due to the formation of matrices by the polymers.[50] In this matrices the target molecules can sit or even forms crystals, by interaction with the polymer interfaces[51], which might affect the selection of polymorphs. Here, two different polymers were used; polystyrene and Poly(mathyl methacrylate).

3.3.1 Polystyrene

Polystyrene is a polymer with semi-crystalline thermoplastic properties, which is widely used, as standard plastics, for instance, as insulating material or as packing material.[52] In Figure 3.4a the structural formula of mono-styrene, one monomer unit of polystyrene, is depicted. Styrene consist of one phenyl ring and one vinyl group. Through polymerisation[53], the vinyl groups break and carbon-carbon bond between other styrene monomers are emerged. Thus, long polymer chains are possible. Hereby, three different arrangement of the chains can be distinguished. The first possibility is a atactic polystyrene, randomization of the vinyl rings. Atactic polystyrene is amorphous. At the syndiotactic polystyrene, the vinyl rings posses a alternating array, thus the polystyrene shows a semi-crystalline behaviour. The last possibility, is the isotactic polystyrene, where the vinyl rings are arranged always on the same side of the polymer chain. Therefore, polystyrene in that conformation forms semi-crystalline structure. For solution and sample preparation atactic polystyrene was used.

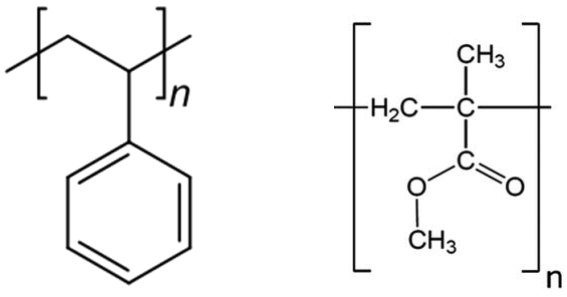

(a) (b)

Figure 3.4: Structural formula of one link from a): the polystyrene chain, b): the PMMA chain

3.3.2 Poly(mathyl methacrylate)

Poly(mathyl methacrylate)(PMMA) is a thermoplastic, which is known by brands like Plexiglas, Acrylite, Lucite and Perspex. The structural formula of the constituent PMMA monomer is shown in Figure 3.4b. Due to the high transparency (transmittance of 92% at 3 mm thickness) and the relative low weight ($\rho = 1.18 \frac{g}{cm^3}$) it is widely used as alternatives to conventional glass.[54] Furthermore, PMMA shows excellent residence against UV-radiation and other environmental influences. The relative low toxicity allows the application of PMMA in the human body. Thus, it can be used as an agent carrier, e.g. in plaster or implants.

Chapter 4

Experimental results

4.1 Ethanol as solvent

In this section the results of all samples prepared by the various methods including drop casting, spin coating and dip coating are summarized.

4.1.1 Films from drop casting

To get a first idea of the crystallization of nabumetone from ethanol, various thin films were produced on glass substrates. For the first sample, a 11 mg/ml solution was prepared and 10 µl were dropped onto glass. The second sample was prepared from a 5.5 mg/ml solution, so half of the first, but 20 µl were dropped onto a glass substrate. This means the liquid amount changed but the amount of nabumetone remained the same. One can calculate that 0.11 mg of nabumetone was hosted at these substrates after solvent evaporation. Another sample hosted again 0.11 mg nabumetone but was prepared from a 2.75 mg/ml solution.
Within all samples the drop showed spreading and the solvent evaporation took about 10 minutes. First crystals were observed already from very early times when prepared from the highest concentrations. For another prepared films crystals could not be identified by eye inspecting.
In Figure 4.1 the optical micrograph of these three samples are summarized. Using the 11 mg/ml solution the nabumetone crystallized into extended needles(Figure 4.1a). The length varies from some hundreds of µm up to cm range. The width shorts at around some µm up to about 200 µm.
Employing crossed polarizer configurations for the optical microscope images shows various bright areas. Such a behaviour typical arises for materials being birefringent which many crystals are. There exist a lot of colour change along the crystals;

thickness changes or defect can result in such changes.
The second sample (5.5 mg/ml solution) shows the formation of a film and on the top of this film small droplets occurred(Figure 4.1c). The size of those droplets varies by a few hundreds µm. Moreover, the density of the film or local thickness of nabumetone changes across the sample which exhibits darker and brighter droplets. The usage of a 2.75 mg/ml solution of nabumetone for sample preparation results again in a thin film and the formation of big grains (Figure 4.1d). In those grains the nabumetone possesses a needle like structure. The width of the grains is up to 5 mm. Between the film and the grain dewetting exist without material being visible.

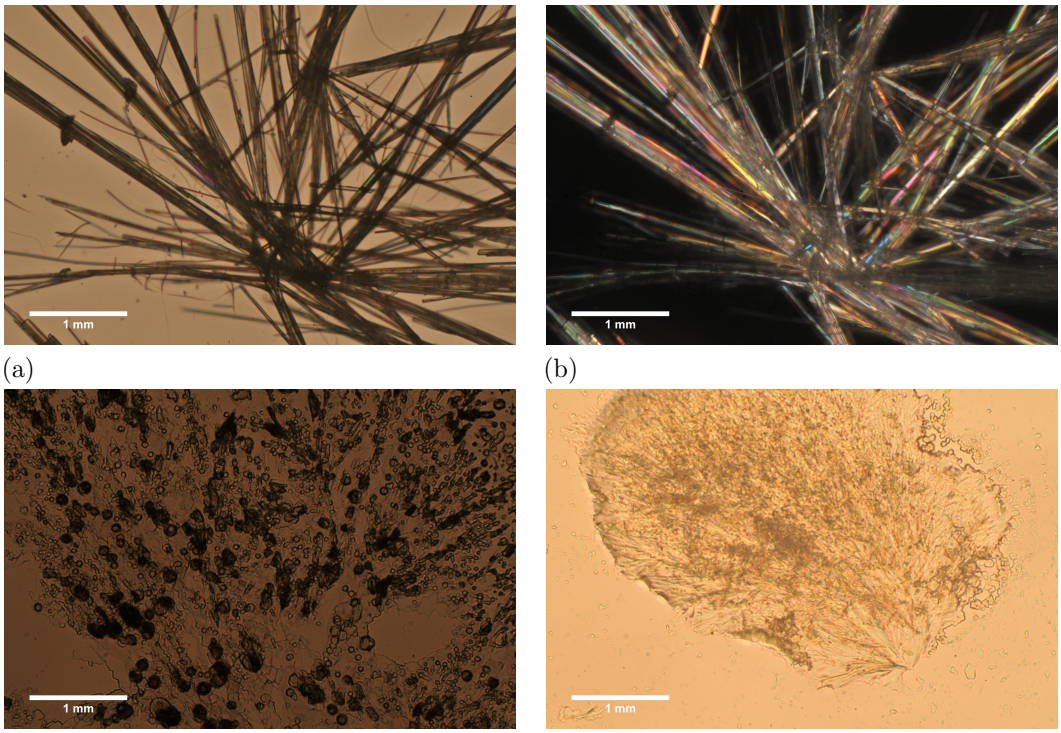

(a) (b) (c) (d)

Figure 4.1: Optical micrographs of drop casted nabumetone films on glass. The concentrations of the ethanol solution and the amount deposited were a): 11 mg/ml 10 μl, b): 11 mg/ml 10 μl polarized, c): 5,5 mg/ml 20 μl, d): 2,75 mg/ml 40 μl.

The X-ray diffraction data for the various drop casted films are shown in Figure 4.2. All data are collected by $\Theta/2\Theta$ scans i.e. specular scans, in the range of 2Θ = 5-30°as this region provide the most important information. The measurement on the sample prepared from the 11 mg/ml solution reveals various peaks distributed over the entire scan range. The most intense are located at 7.95° and 24.07°. The comparison of the measured peak position with theoretical positions of the various nabumetone polymorphs reveals that all those peaks are a result of the thermodynamic stable

nabumetone form 1. As there are many peaks visible this further shows that this sample behaves like a powder. Comparing the relative peak intensities with those of an ideal powder reveals that a slight preferred orientation exists.
In the X-ray pattern of the sample from the 5.5 mg/ml solution the powder like behaviour of the first sample is not observed. High intense peaks lies at 7.95° and at 21.47°. Those two peaks belongs to polymorph 1 and indicate 10-2 and 204 texture. Furthermore, some other peaks have a lower intensity compared to the 11 mg/ml sample too. Beside the form 1 peaks additional peaks at 6.49° and 9.76° appears, which are the result of metastable nabumetone polymorph 2 and indicate a 100 texture of the second form on the sample.
The X-ray data from the third sample, which was prepared from a 2.75 mg/ml solution, reveals only few peaks with the most intense located at 21.47°, which belongs to the (204) plane of nabumetone form 1. The two peaks at 6.49° and 9.76° belong again to the metastable form 2 of nabumetone.

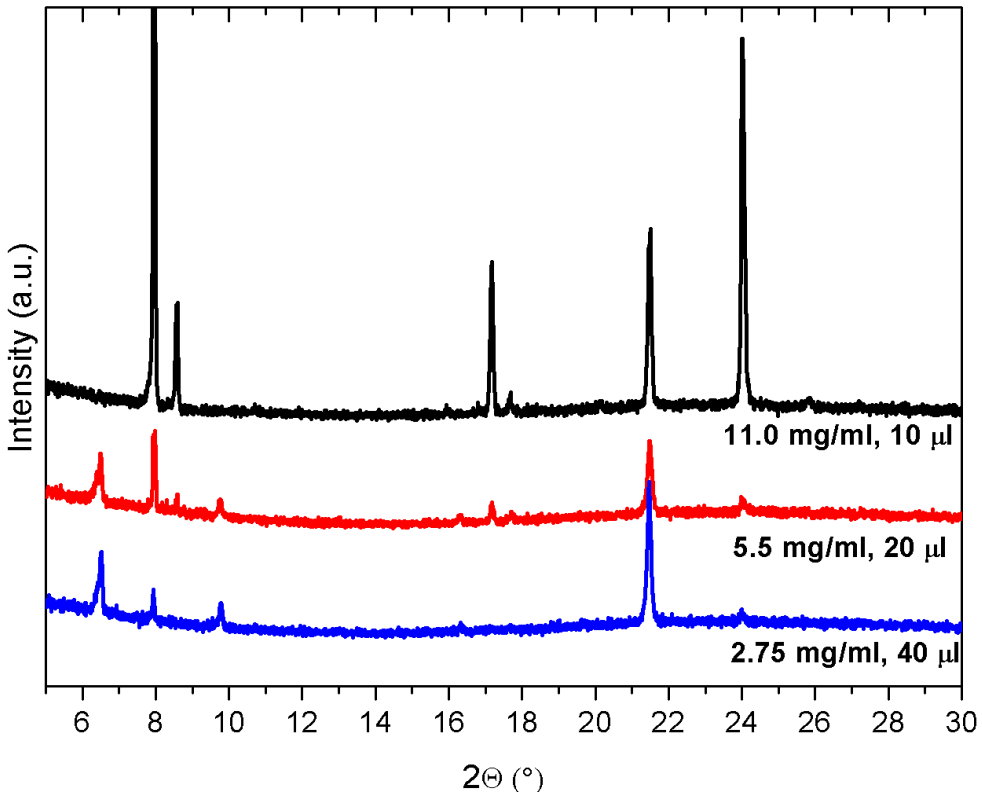

Figure 4.2: Specular X-ray diffraction data of drop casted from nabumetone/ethanol solutions on glass employing different concentrations and amounts, Curves are shifted for clarity.

To study the impact of the evaporatin times on the crystallization, samples were covered using a petri dish. This resulted in the atmosphere of the solvent around the

sample to solvate to a higher degree, but also the time for the solvent evaporation increased drastically. To test the differences, a sample series similar to above was prepared, i.e. the concentration was halved while the amount of solution was doubled. The X-ray data of the 15 mg/ml sample reveal 3 peaks which are located at 7.95°, 21.47°and 24.07°. The absence of the other peaks mean that a certain degree of textures is present in this sample. The peaks can all be addressed to form 1 of nabumetone. Reducing the concentration, the behaviour remains very similar, with all peaks corresponding to form 1. Please note that at a concentration of 5.5 mg/ml a fast solvent removal resulted in the formation of a significant amount of form 2. The lowest amount tested reveals a single texture of 204 (Figure 4.3a).
In Figure 4.3b X-ray data for three samples prepared from a 7.5 mg/ml solution but with various amounts of deposited material and covered after the deposition are depicted. At 40 µl one intense peak located at 21.49° corresponding to the 204 peak of form 1 is observed. Furthermore, other peaks resulted from nabumetone form 2 are present. Those form 2 peaks disappeared by the deposition of 20 µl, the half of the previous sample, and only three form 1 peaks were observed. Further halving of the deposited amount resulted in low intense peaks, compared to higher deposited amounts. Here, again both forms of nabumetone with corresponding peaks were obtained. Thus, the second sample does not follow the trend of the others.

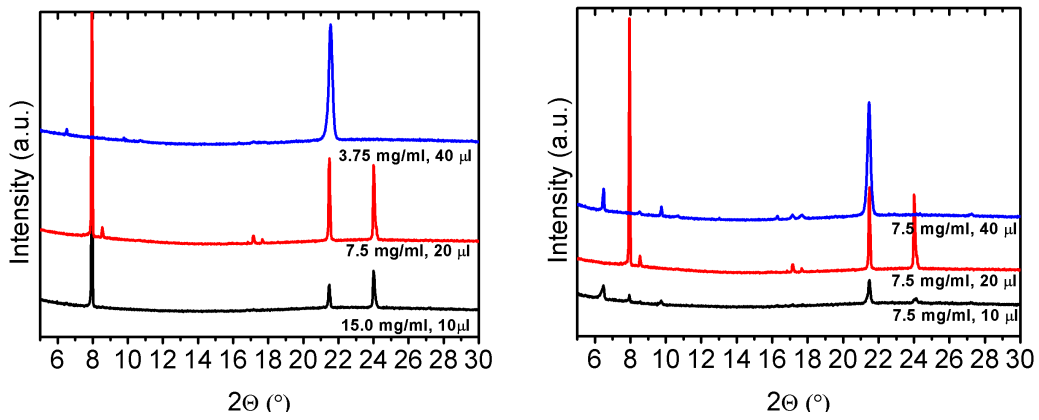

(a) (b)

Figure 4.3: Specular X-ray diffraction data of drop casted and covered nabumetone/ethanol films on glass from solutions of a)different concentrations and amounts b) a concentration of 7.5 mg/ml and different amounts, Curves are shifted for clarity.

4.1.2 Drop casting on polystyrene

The previous section depicts how the nabumetone/ethanol concentration and its amount influence the shaping of the crystal structure. In this section it is shown how the nabumetone crystallizes on a polystyrene surface. For this issue polystyrene had to deposited on the silicon substrates via spin coating rather than on a bare glass substrate As solvent for the polystyrene solutions toluene was used. The concentrations of the polystyrene (PS) solutions were 7 wt.% and 4 wt.%. After the evaporation of toluene the nabumetone/ethanol solutions were deposited via drop casting onto these PS-surfaces.

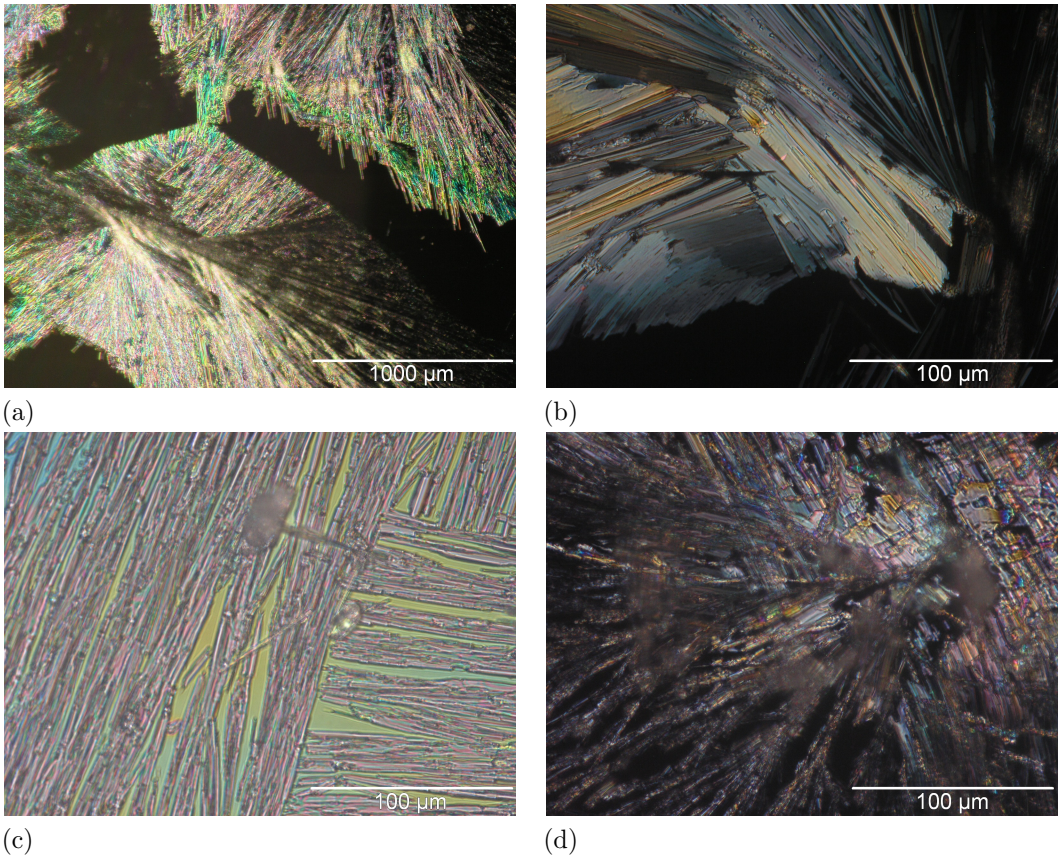

(a) (b) (c) (d)

Figure 4.4: Images from optical microscope measurements of drop casted nabumetone/ethanol films on polystyrene surfaces from different concentrations of polystyrene/toluene solutions, a): 2.75 mg/ml on a 4 *wt.*% polystyrene surface polarized, b): 2.75 mg/ml 7 *wt.*% polystyrene polarized, c): 5.5 mg/ml on 4 *wt.*% polystyrene, d): 5.5 mg/ml on 7 *wt.*% polystyrene polarized.

In order to get the less stable polymorph 2 on the surface, those concentrations from the drop casted films were chosen, where crystallization of polymorph 2 was observed on glass. Thus, concentrations of 5.5 mg/ml and 2.75 mg/ml were used. In

Figure 4.4 the recorded images from the light microscope are shown.
The films produced by drop casting on polystyrene differs from those on glass (c.f. Figure 4.1). Especially the formations of droplets readily present on glass with concentrations of 5.5 mg/ml and 2.75 mg/ml disappear and little needles are formed on polystyrene. Moreover, those films seem on the one hand to be smother on PS, and on the other hand they have a preferred directions in which the needles growth.
The specular X-ray diffraction results for the on PS drop casted films between $2\Theta = 5°$ and $30°$ are depicted in Figure 4.5. At a concentration of 2.75 mg/ml the nabumetone form 1 204 texture appears with a strong peak at $2\Theta = 21.49°$ of both PS concentrations. The differences between 4 $wt.\%$ and 7 $wt.\%$ is shown in the lower intensity of the (204) peak and the absence of low intense peaks.
Contrary, the 5.5 mg/ml films crystallize in two different textures. On the 4 $wt.\%$ PS surface nabumetone forms a 10-2 texture of polymorph 1 with a strong peak at $2\Theta = 7.95°$ and on the 7 $wt.\%$ PS surface the form 1 (204) peaks becomes stronger, whereas, the (10-2) peak has a very low intensity.

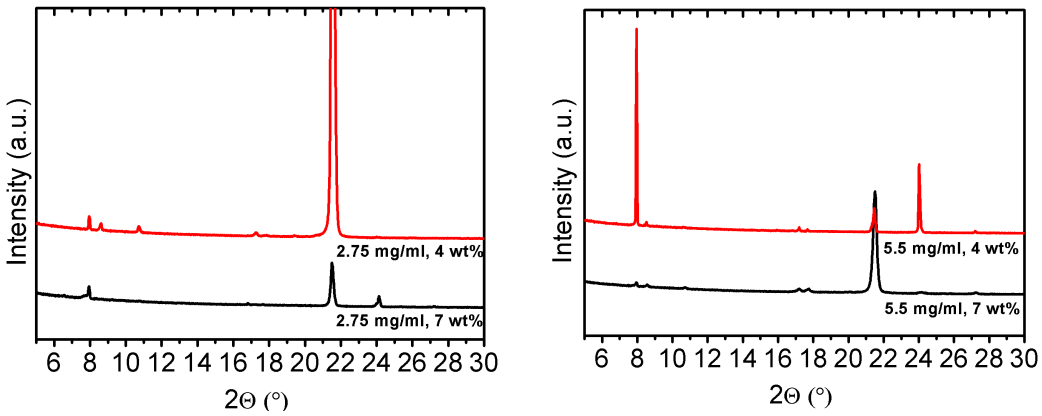

(a) (b)

Figure 4.5: Specular X-ray diffraction data of drop casted nabumetone/ethanol films on PS surface from PS/toluene solutions with two different concentration of 7 wt.% and 4 wt.% a): with a concentration of 2.75 mg/ml b): with a concentration of 5.5 mg/ml.

4.1.3 Films from spin coating

To get thinner and more homogeneous films prepared from nabumetone/ethanol solutions the spin coating technique was applied. As substrates glass and native silicon wafers were used. Figure 4.6 depicts the nabumetone thin films on silicon substrates. A nearly saturated nabumetone/ethanol solution of 20 mg/ml was used to get a higher amount of nabumetone on the substrate. Figure 4.6a exhibits crystals obtained after spin velocity of 10 rps. These crystals have the form of islands or mounds and seem to be homogeneously distributed over the whole silicon surface. The polarized image at higher magnification (Figure 4.6b) shows that the islands/mounds are probably crystalline and have width between 10 and 30 µm. Using a faster velocity of 20 rps results in a decrease of island sizes and in a finer distribution of the islands over the silicon surface(Figures 4.6c, 4.6d).

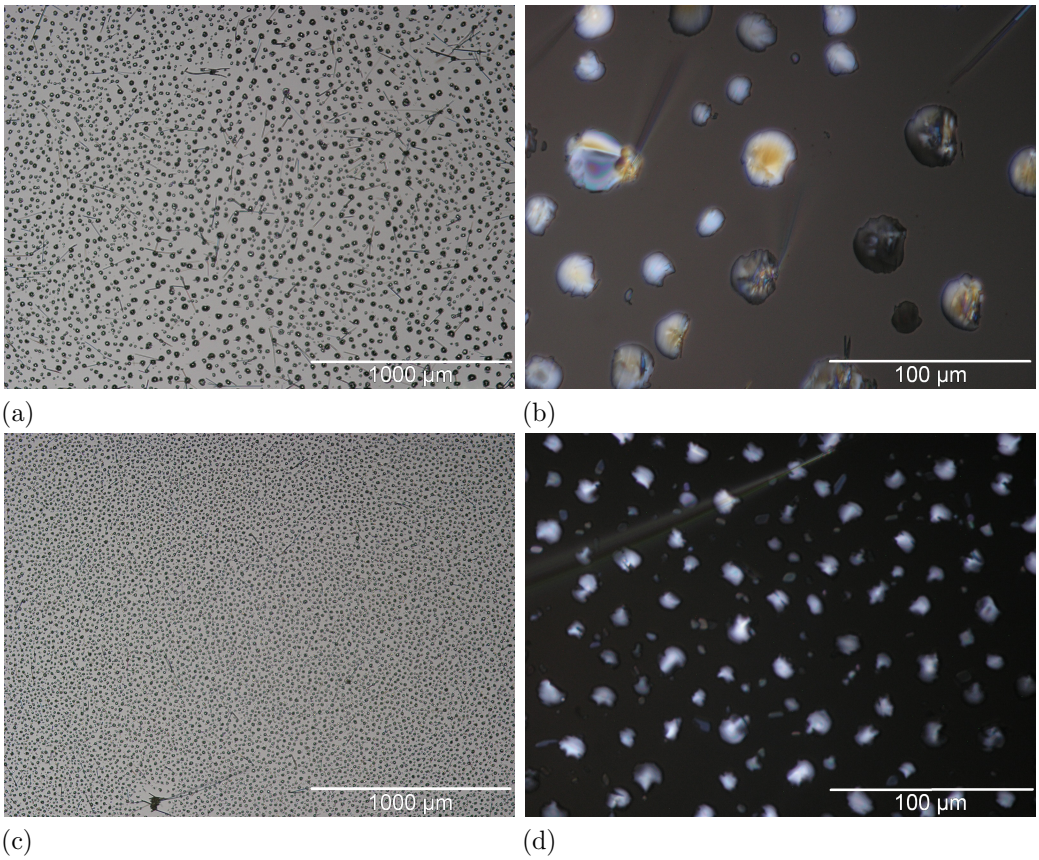

(a) (b)

(c) (d)

Figure 4.6: Light microscope images from a 20 mg/ml nabumtone ethanol solution processed by spin coating on native silicon. a): Image of 10 rps spin coated film , b): Polarized images of a) at higher magnification, c): Image of 20 rps spin coated film, b): Polarized images of c) at higher magnification.

Comparing the two polarized images (4.6b, 4.6d) indicates that the islands formed

by higher spin velocities are indeed smaller than those from 10 rps. They also do not have any longer the round shape but are more edged. As shown in Figure 4.6 the choice of the spin velocity has an influence on the distribution and the shape of the islands on the surface. Higher spin velocities result at first in smaller islands but the size stays constant by higher velocities than 40 rps. The island shape transform from drop mound shape to a plate shape. The use of different substrates (glass or native silicon), which is not shown here, have no influence on the crystallisation.
The specular X-ray diffraction results for both velocities of the spin coated 20 mg/ml solution films (Figure 4.7) exhibits a 100 texture of polymorph 2 with peaks at $2\Theta = 6.51°$, 9.77°, 13.01°, 16.31°and 19.62°. The film produced by 10 rps has also an additional peak at $2\Theta = 21.5°$, which corresponds to the (204) plane of polymorph 1. But as this is very small it follows that this is the minority species. At 20 rps that peak does not exist. It is shown that the form 2 peaks become less intense by applying a higher spin velocity. Furthermore, additional peaks appear near by the 2n00 peaks (200, 400, 600) of form 2. Moreover the 400 peak and the 600 peak are much weaker in intensity than the following peaks of 300 and 500 directions. These peaks belong to a new unknown phase as will discussed below.

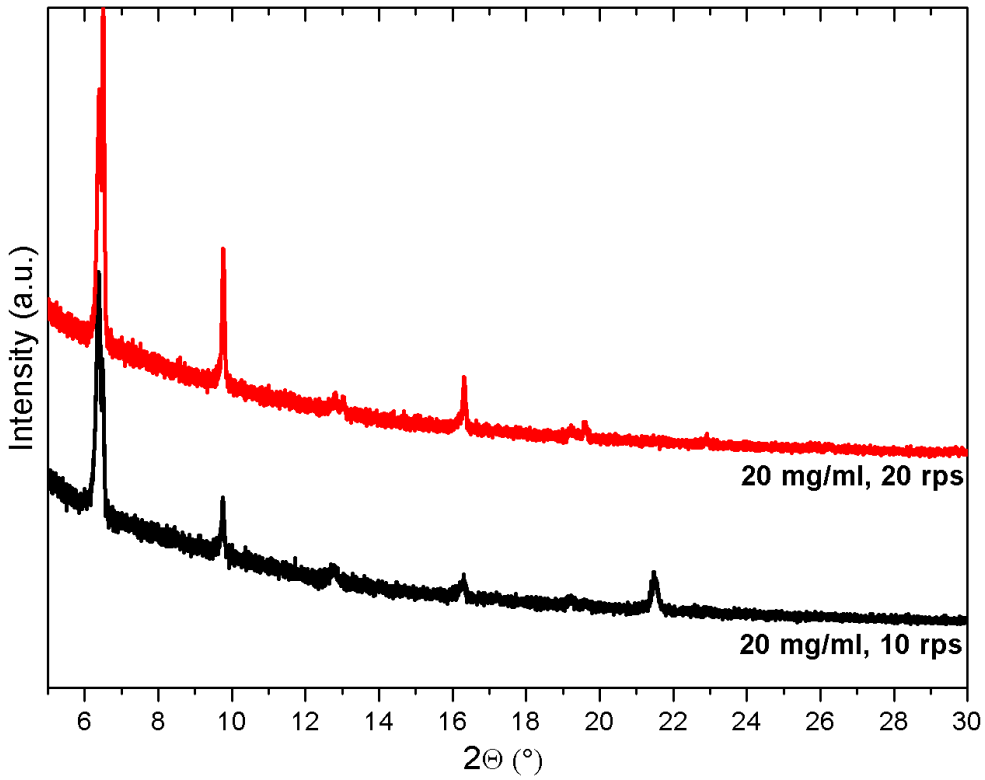

Figure 4.7: Specular X-ray diffraction data spin coated 20 mg/ml nabumetone ethanol films prepared at 10 rps and 20 rps.

In the next Figure 4.8 XRD results of spin coated films for different concentrations are shown. Thus, the influence of concentrations on the crystallisation of nabumetone is evaluated.

At all four tested concentrations polymorph 2 crystallizes in a 100 texture with an inter-planar distance of 27.30 $\mathring{A}$. The measurement on the sample prepared from the 7 mg/ml nabumetone/ethanole solution reveals that the (204) peak of stable polymorph 1 also formed beside the peaks of metastable polymorph 2. Again all scans reveal double peaks, which are located near by the known 2n00 peaks of form 2. The intensities of these additional peaks, especially that one at the (200) peak varies with different concentrations. Lower concentrations show a decrease of the first double peak.

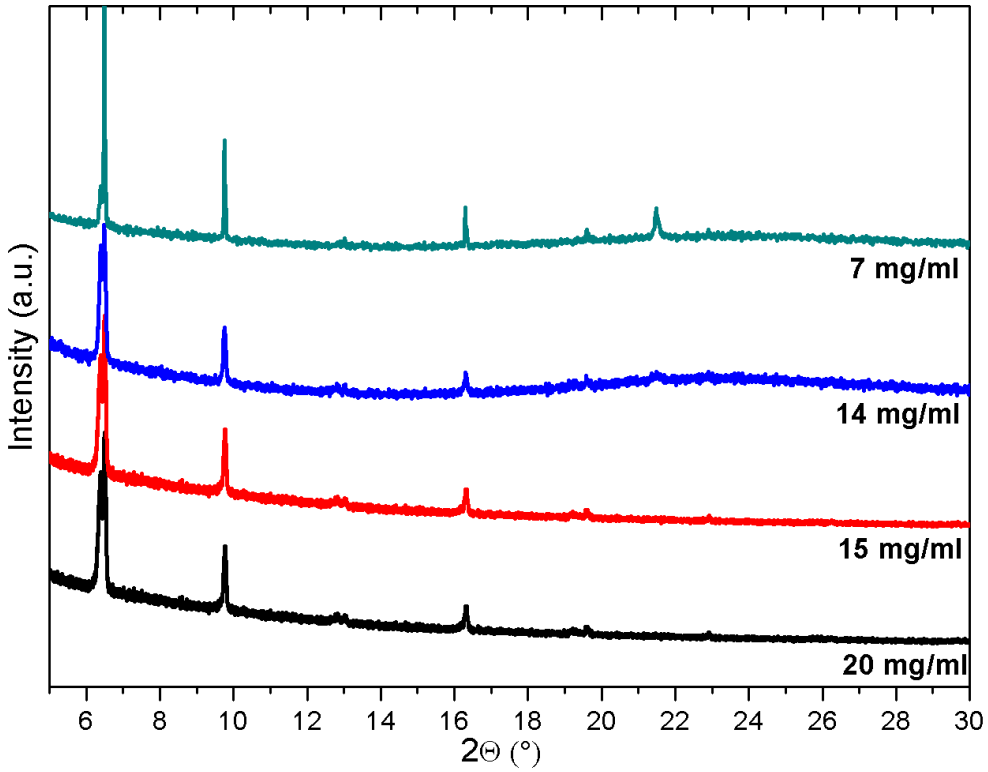

Figure 4.8: Specular X-ray diffraction data of spin coated nabumetone/ethanol films at different concentrations. All samples were prepared at 20 rps. Curves are shifted for clarity.

After investigating the influence of the concentrations on the crystallization, the influence on the spin velocity is analysed. Figure 4.9a shows the specular XRD data for spin coated films at velocities of 10 rps, 30 rps 50 rps and 70 rps. The used concentration for those experiments was 15 mg/ml. It is obvious from the absence of specific peaks that polymorph 1 is not formed on the glass substrate for any of the

velocities, but form 2 crystallized with the known peak located at 6.51°, 9.77°, 13.01°, 16.31°and 19.62°. Additional the new form appears with the same peak positions known from previous results.

A closer inspection the double peaks at $2\Theta = 6.51°$ is depicted in figure 4.9b. The result for 10 rps shows that the peak of the unknown form at 6.39° is more dominant than that of the known phase 2 at 6.51° which is only reflected in a shoulder of the dominant peak. Calculation of the intet-planar distance resulted in 27.75 $\AA$. Higher spin velocities display on one hand the formation of a stronger peak of the known phase and on the other hand the decrease of the peak from the unknown phase. At 70 rps both peaks have the same intensity. It should be noted that higher ordered double peaks reveal the same behaviour.

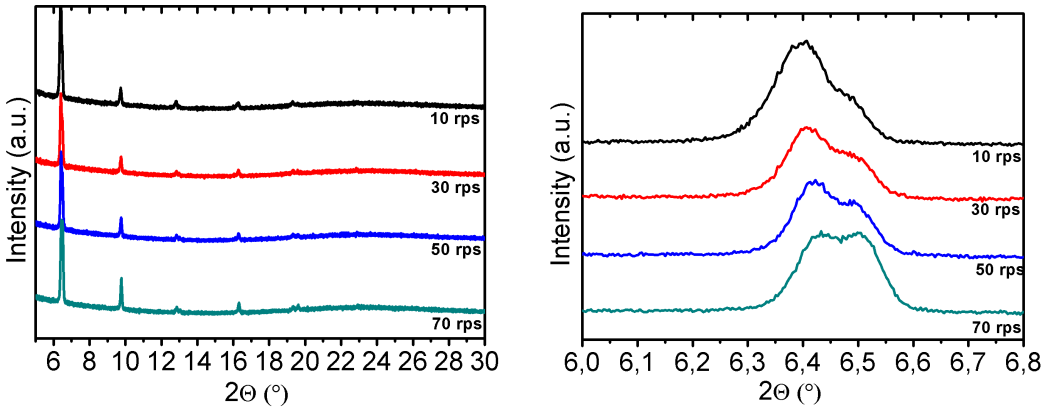

(a) (b)

Figure 4.9: Specular X-ray diffraction data of spin coated 15 mg/ml nabumetone/ethanol as function of spin velocities (a) and higher resolution image of the double peaks at 2Θ =6.5° and 6.4° (b).

To get films containing a higher ratio of polymorph 2 on the substrate the spin coating process is varied. The previous films were produced by depositing at first the solutions on the substrates and starting the spin coater in the next step. The modified technique differs in the sequence of the process. At first the spin coater is started and then the solution is deposited. That technique is called, to distinguish from the other, dynamical spin coating.

The specular XRD results from the dynamical spin coating at different velocities show similar pattern to those of the normal spin coated samples(Figure 4.10). For all three velocities polymorph 2 with a 100 texture is crystallized with peaks located at the same positions known from previous measurements. The increase of the spin velocity result here in an increase of the peak intensities.

Figure 4.10b exhibits the spin velocity influence on intensities of the peaks, which

are located at 6.39°and 6.51°, applying dynamical spin coating. The peak at 6.39° is at first stronger than the peak at 6.51°. Contrary to Figure 4.9 the variation of the spin velocity influences the intensity change much stronger. At 30 rps both peaks are equal intense and at 50 rps the (200) peak of form 2 dominates. Pure form 2 was not discovered with the tested speeds. Likely following the trend form 2 might be the only phase when much higher spin velocities are used.

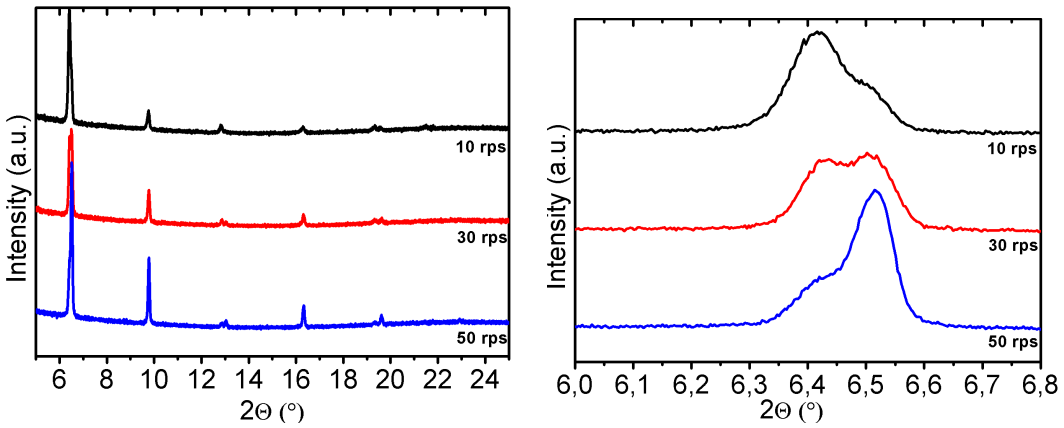

(a) (b)

Figure 4.10: Specular X-ray diffraction data of dynamical spin coated 15 mg/ml nabumetone/ethanol films on glass a): by different spin velocities b): higher resolution image of the double peaks at 2Θ =6.5° and 6.4°.

Various test on different compinations in the spin coating process had been tested. The reuslts show the choice on the substrate, glass and native silicon, does not play a role for crystallisation from spin coating.

Grazing incidence X-ray diffraction

Grazing incidence X-ray diffraction (GIXD) measurements were performed at the Elettra Synchrotron Trieste to get not only information in the specular direction but also in-plane. Figure 4.11 shows a typical GIXD result for a 20 rps spin coated film from a saturated nabumetone/ethanol solution together with calculated Bragg peaks. The angle of incidence was set to α_i =1.7°.
The 100 texture of polymorph 2 is shown by peaks in specular direction, q_{xy} =0 $\mathring{A}^{-1}$. Those peaks were also observed in the measured specular X-ray diffractograms. Due to mosaicity peaks are smeared out along the Debye-Scherrer rings.
The peak at $q_{xy} = \pm 1.6$ $\mathring{A}^{-1}$ and q_z =1.2 $\mathring{A}^{-1}$ belongs to the used silicon substrate (111) plane. In plane the intense 111 peak of polymorph 2 is observed beside low intense peaks of the directions of 202, 302 and 312. The calculated peaks fit well to the experimental results.
Unfortunately the new phase can not be clearly identified due to the fact of the low resolution. Changing the angle of incidence to higher angles yields admittedly to smaller peaks but the resolution was still to small to see the new form.

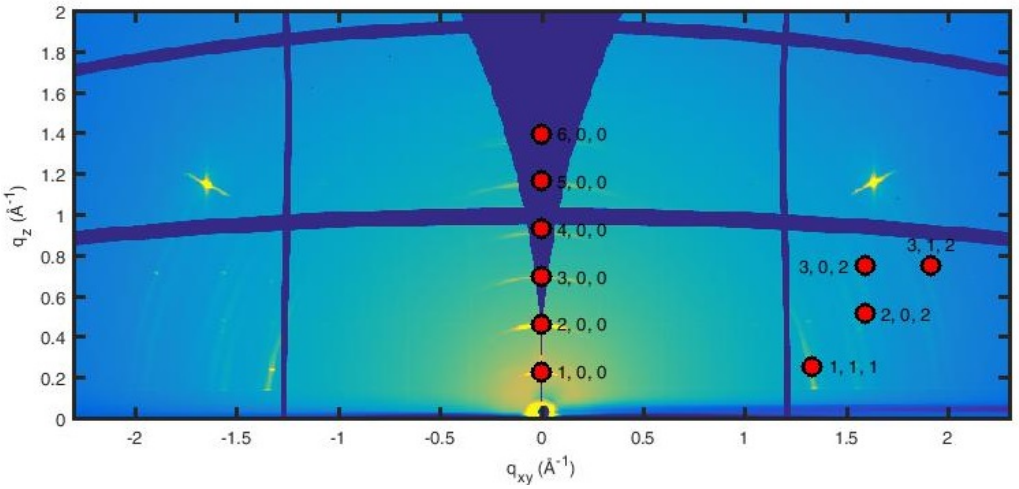

Figure 4.11: Grazing incidence X-ray diffraction map from measurements of 20 rps spin coated 20 mg/ml nabumetone/ethanol film, the red cycles describe calculated bragg peaks from *GIDVis*.

4.1.4 Films from dip coating

Dip coated films were made out of different nabumetone/ethanol solution and different withdraw velocities. In Figure 4.12 some optical microscope images are depicted. It shows the crystallized nabumetone films produced at withdraw velocities of 5 μm/s and 10 μm/s. The used concentration was 15 mg/ml.
The results show that needles crystallized onto the native silicon sample produced at a withdraw speed of 5 μm/s. Compared to samples produced by drop casting (Figure 4.1a), it seems that these needles are formed by the stable polymorph 1. The difference between drop casting and dip coating is, that for dip coating the needles are formed along preferred direction, which growth in the opposite direction of the withdraw. Moreover, some small needles built cross links between the larger ones.
Applying a higher withdraw velocity leads to a thicker film, which still shows the directed needles. The space between those needles is now filled by very thin needles. Those needles seem to crystallize on the edges of the bigger needles and have no specific growth direction.

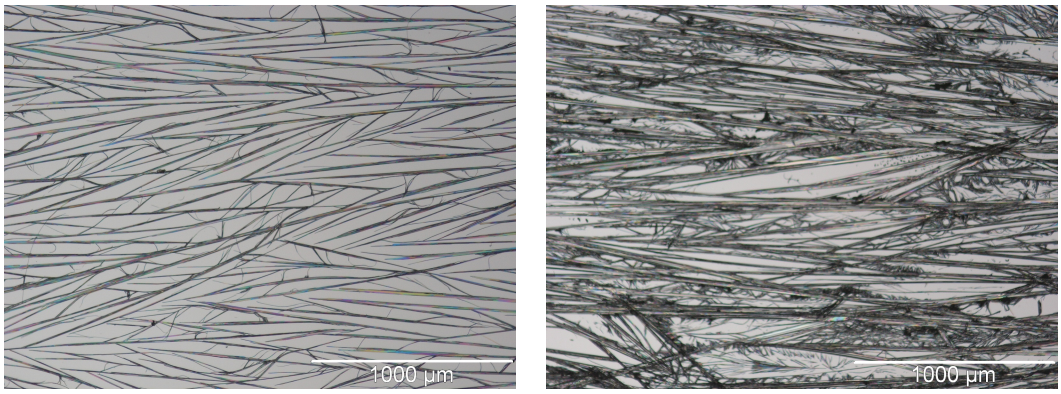

(a) (b)

Figure 4.12: Samples prepared via dip coating out of a 15 mg/ml nabumetone/ethanol solution with a withdraw velocity of a): 5 μm/s and b): 10 μm/s.

Figure 4.13 exhibit the results of the Θ/2Θ-scans between 6° and 30° for samples produced with two different withdraw velocities. The measurement on the sample prepared with a withdraw speed of 5 μm/s shows two strong peaks located at 7.95° and 21.49°, with some additional less intense peaks in between. That data yield to two different and dominant orientations of the stable polymorph 1 on the substrate.

By contrast the data of the sample with a withdraw velocity of 10 μm/s indicates specific orientations with two more high intense peaks. The peaks at 2Θ =8.57°and 17.18° belongs to the (200) and the (110) planes of nabumetone's form 1.

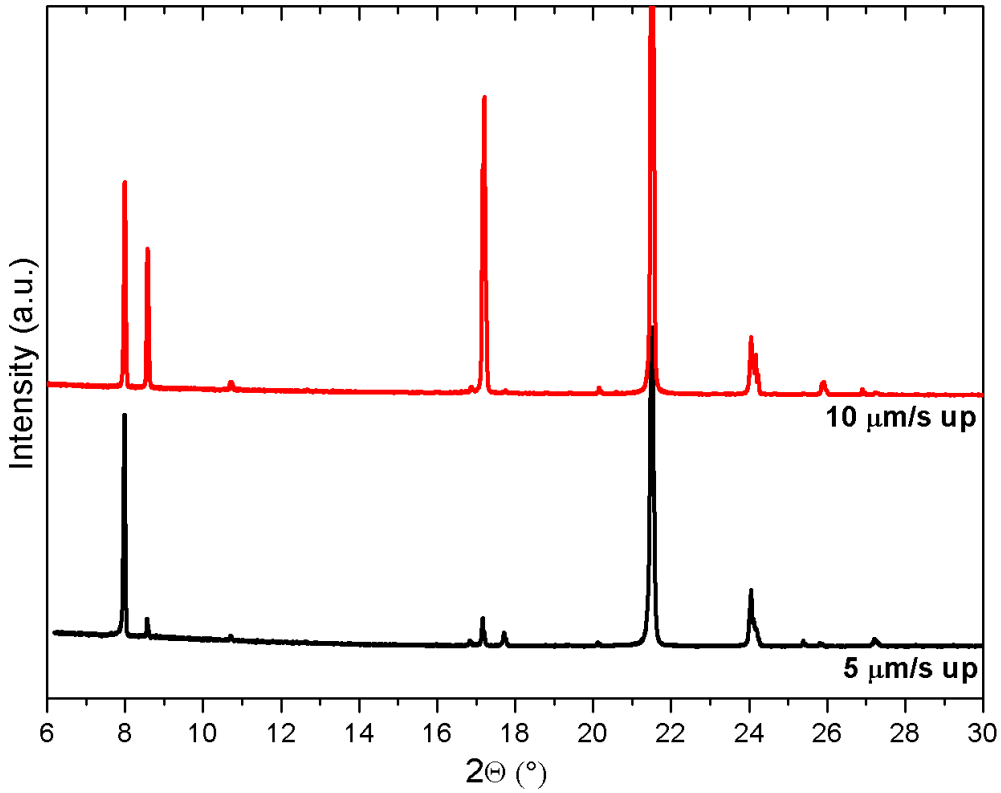

Figure 4.13: Specular X-ray diffraction results for dip coated films from a 15 mg/ml nabumetone/ethanol solution with a withdraw velocity of 5 μm/s and 10 μm/s.

4.2 Stability test of nabumetone

The stability is a big issue for the investigation of polymorphic structures. Due to the lower stability, polymorph 2 recrystallize for some reason to polymorph 1. That mechanism was observed for different samples, but mainly on spin coated films, where polymorph 2 was primarily formed.
Figure 4.14 exhibits results from specular X-ray diffraction scans of such a recrystallisation for a spin coated film prepared from a 14 mg/ml solution. The first investigation was made one week after the preparation, the second after 1 month. At first, both the new form and polymorph 2 with a 100 texture was observed. 1 month later the remeasurement showed that the peaks of form 2, especially the (200) peaks, disappeared, while the (10-2) and the (204) appeared on the surface.

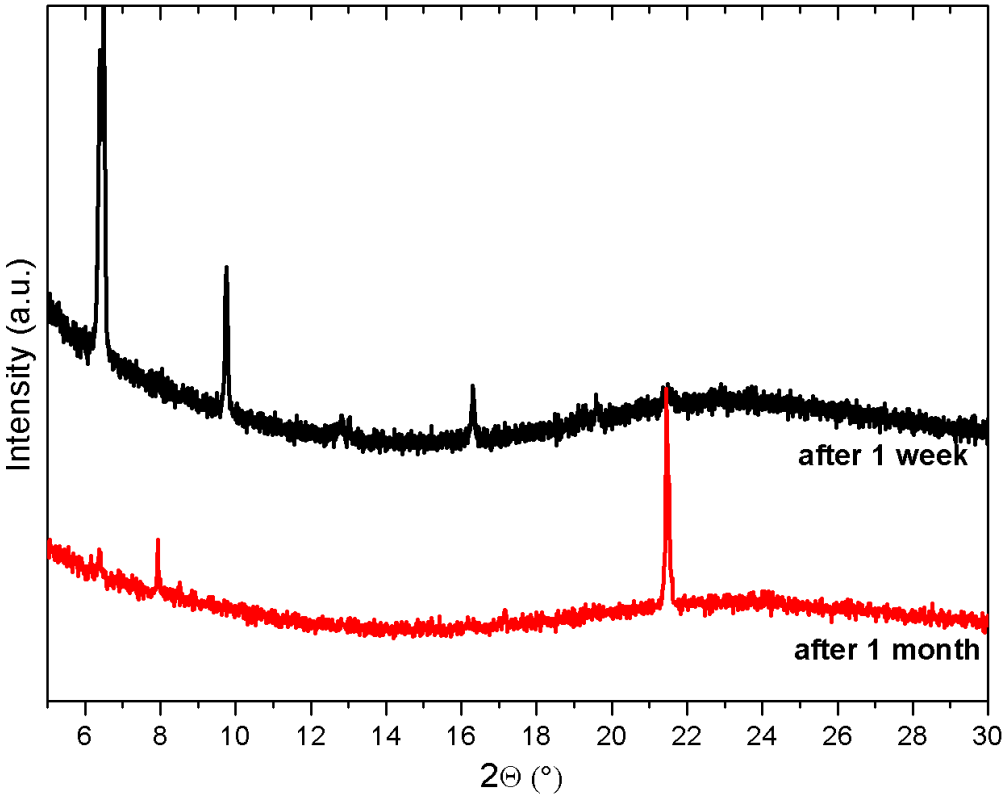

Figure 4.14: Specular X-ray diffraction data of the same spin coated nabumetone film after 1 week and 1 month of production.

For a better understanding specular XRD heating data were provided by Christian Röthel for spin coated nabumetone/ethanol solutions. The first experiment was an annealing experiment with the goal to determine the melting point of polymorph 2, thus the temperature starting at 35 °C was increased every 2 minutes by 5 °C and

a $\Theta/2\Theta$ scan between 2Θ =5° and 9° was taken after the increase (Figure 4.15a). At first the (200) peak of polymorph 2 at 2Θ =6.5° is observed. By reaching a temperature between 65 °C and 70 °C the melting point was reached and polymorh 2 started to form polymorph 1 and the intense (10-2) and the (200) peaks appeared. After cooling back to room temperature polymorph 2 did not appear again.
In the second experiment the sample were heated to a temperature above the melting point of polymorph 1 and was than cooled down to room temperature. Starting with 70 °C only the form 1 (10-2) peak is present. At 80 °C the melting point of form 1 was reached and this peak disappeared leaving a empty pattern. After reaching 90 °C the sample was cooled down to room temperature. At about 50 °C the form 2 (200) peak at 6.5° appeared again. Thus, polymorph 2 started to crystallize from melt.

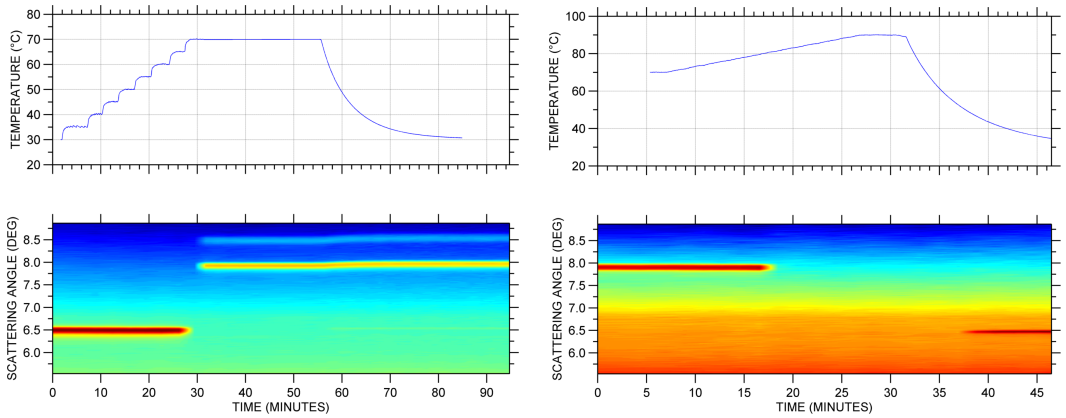

(a) (b)

Figure 4.15: Heating experiment of spin coated nabumetone ethanol film. a): annealing polymorph 2 up to 70 °C b): heating form 1 up to 90 °C with each cooling back to room temperature.

4.3 Tetrahydrofuran(THF) as solvent

4.3.1 Thin films from spin coating

Spin coated thin films from a nabumetone/THF solution were prepared on bare silicon substrates at different concentrations. The spin velocity was set to 30 rps. Figure 4.16 depicts the light microscope images for concentrations of 100 mg/ml, 25 mg/ml, 6.25 mg/ml and 3.12 mg/ml. The film produced from a 100 mg/ml nabumetone/THF solution shows the formation of spherulites on the surface. Spherulites have a middlepoint where they starts to crystallize mostly as needles. Interesting here are the different textures, which are formed in the grains. For example, the spherulite in the middle has smaller and not highly directed needles. The surrounding spherulites have a more needle like structure. The width of the spherulites varies between 1 mm and 2 mm, which depends how fast the surrounding spherulites growth.

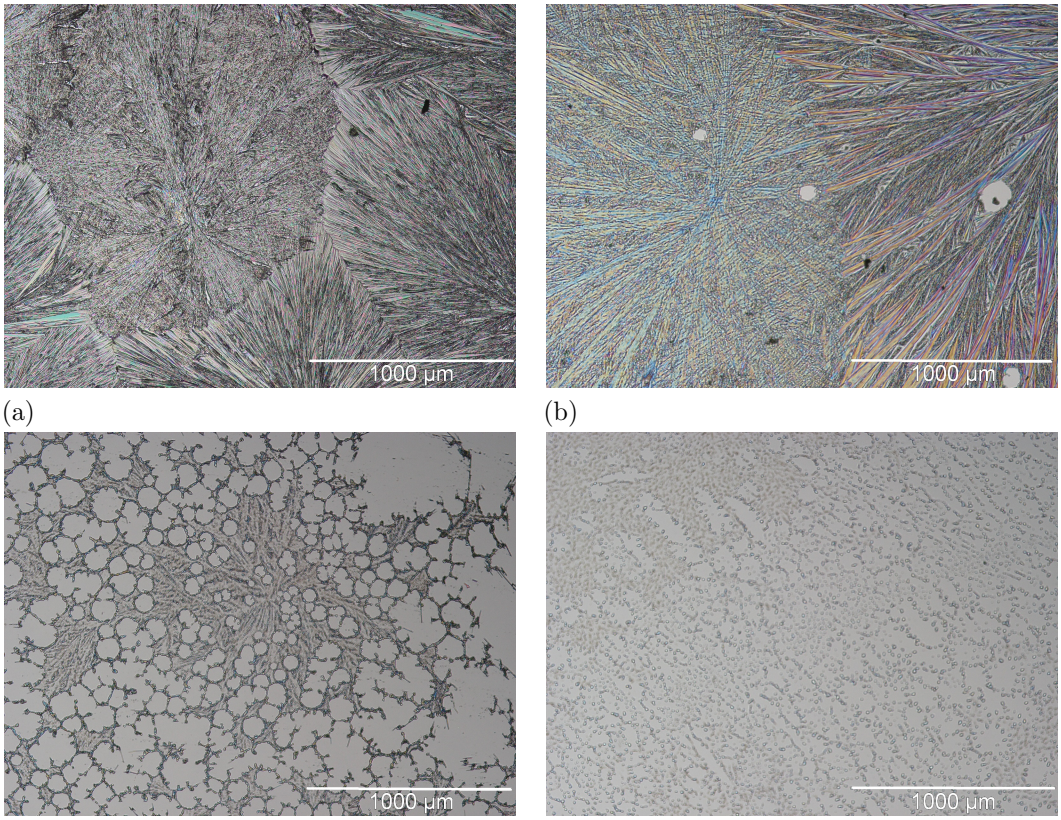

(a) (b)

(c) (d)

Figure 4.16: Optical microscope images of various spin coated nabumetone/THF films on native silicon prepared with an amount of 50 μl and a velocity of 30 rps, The concentration varied by a): 100 mg/ml, b): 25 mg/ml, c): 6,25 mg/ml; d): 3,12 mg/ml.

The image of the sample produced out of a concentration of 25 mg/ml (Figure 4.16b) shows two large spherulites. In the left spherulite the needles are much finer, than in the right spherulite, where big directed and small needles are crystallized. Additionally some dewetting area are observed in both spherulites.
At a nabumetone/THF concentration of 6.25 mg/ml the spherulites are not observed any more. Figure 4.16c exhibits a strong increase of dewetting on the silicon substrate. At the grain boundaries plate shaped islands formed and in between some needles were crystallized.
The thin film made from a 3.12 mg/ml nabumetone/THF solution shows only the crystallisation of small islands. The islands/mounds have an homogeneous distribution over the entire substrate surface. The dewetted still occur, but with a more stretched layout.

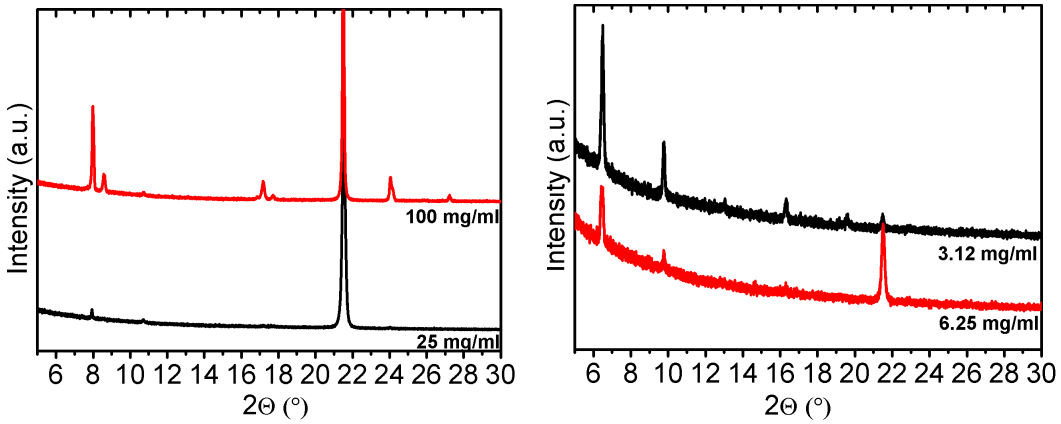

(a) (b)

Figure 4.17: Specular X-ray diffraction results for spin coated nabumetone/THF thin films at a): high concentations and b): low concentrations.

Specular X-ray diffraction scans were made between 2Θ of 5°and 30°. The results are depicted in Figure 4.17. The X-ray scan for sample prepared from a 100 mg/ml nabumetone/THF solution reveals various polymorph 1 peaks. Those different peaks indicates a powder like behaviour with a slight preferred orientation on the substrates. The strongest peak is observed at $2\Theta = 21.49°$ and corresponds to the [204] direction. Other peaks indicate a 10-2 orientation with appropriate angles at 7.95°and the third order 24.01°. At low intense peaks corresponds to polymorph 1 planes ((200), (110), (302)).
The measurement of the film produced with a 25 mg/ml concentrated solution shows, that the powder like structure disappeared and one strong peak at the (204) position can be observed. Another weak peak, belonging to the (10-2) plane also is formed.

In contrast to high concentration thin films, nabumetone solved in THF at a concentration of 6.25 mg/ml forms not only the stable polymorph 1, with a peak located at 21.49°, but also the metastable polymorph 2 with an 100 texture. Near to the (200) peaks at $2\Theta = 6.51°$ a second peak appeared at 6.39°, which belongs to the unknown polymorphic phase found previously (see section 4.1).
The 204 texture of polymorph 1 almost disappeared for a nabumetone concentration of 3.12 mg/ml. Whereas, peaks at $2\Theta = 6.51°$, 9.79°, 13.01°, 16.34° and 19.63° indicating the polymorph 2 100 texture on the thin film developed much more significantly.

The preparation of samples from the same concentrations but with different spin velocities reveals that no change in the polymorphic selection took place by varying the spin velocity. At high concentrations only polymorph 1 was observed and at very low concentrations only polymorph 2.

4.3.2 Composite nabumetone-Poly(methyl methacrylate)

Poly(methyl methacrylate)(PMMA) were used as a polymer matrix and as a crystallisation inhibitor for nabumetone. To avoid side effects due to different solvents both, nabumetone and PMMA was dissolved in THF, because ethanol and toluene solved PMMA in a unsatisfactory way. The prepared PMMA/THF solution had a concentration of 7 wt% . The used nabumetone/THF concentrations were varied between 100 mg/ml, 50 mg/ml, 25 mg/ml and 12.5 mg/ml. Both solutions were mixed at a ratio of 1:1 together and were deposited on native silicon wafer via spin coating and the spin velocity was set to 30 rps. In Figure 4.18 the optical micrographs of those samples are summarized. The nabumetone from the mixture of 100 mg/ml solution and the PMMA solution crystallized in long plates(Figure 4.18a). Those plates lies very tight to others plates and form a film onto the PMMA surface, which can be seen as a colourful background. Moreover, some island crystallized onto the plate film. The length of the plates varies from some hundreds of µm down to a few µm. The island on the top have a size of about 5 µm.

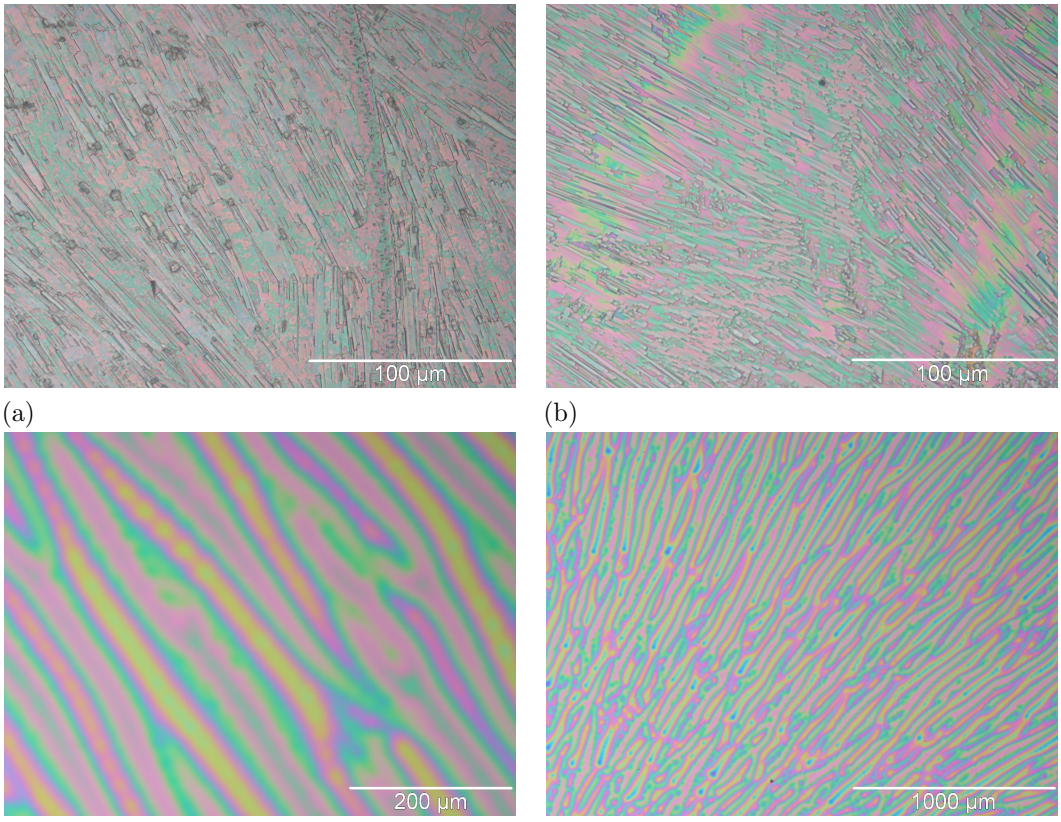

(a) (b)

(c) (d)

Figure 4.18: Optical micrographs of spin coated nabumetone/PMMA (7 wt.%) films on native silicon, the concentrations used for preparation are a): 100 mg/ml, b): 50 mg/ml, c): 25 mg/ml, d): 12.5 mg/ml.

At the second sample, which was made from the 50 mg/ml nabumetone solution, the nabumetone formed again plates on the PMMA surface (Figure 4.18b). Contrary to the previous sample no islands can be observed onto the plate surface. The width of the plates lies between 100 µm and and 10 µm.
The usage of the 25 mg/ml and the 12.5 mg/ml solution in a mixture with PMMA for thin films formation shows that no crystals were formed on the samples investigated by light microscopy. Figure 4.18c and figure 4.18d only depict a colourful background proceed from the PMMA.

The specular X-ray diffraction data for spin coated nabumetone/PMMA films are shown in Figure 4.19. The measured sample produced from 100 mg/ml nabumetone/PMMA mixture reveals a strong peak located at 21.49°. This peak belongs to the stable polymorph 1 (204) plane. Beside the strong peak some low intense but broad peaks can be observed at 6.51° and 9.79°. Those peaks are a result of nabumetone polymorph 2 ((200) and (300) plane)). The broadness of this peaks means that those result from thin crystals.

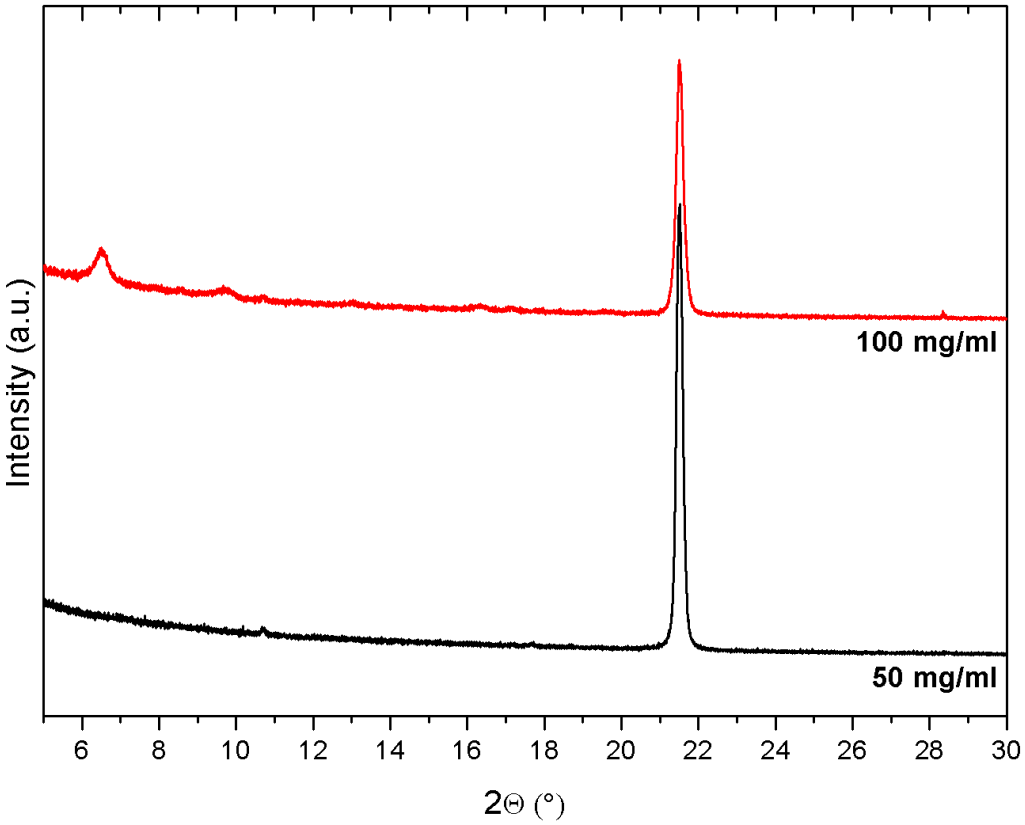

Figure 4.19: Specular X-ray diffraction data of spin coated nabumetone/PMMA films on native silicon from solution with different concentrations.

The second pattern in Figure 4.19 reveals the result of the sample prepared from the 50 mg/ml nabumetone solution mixed with 7 wt.% PMMA. Here only one peak at $2\Theta = 21.49°$ can be observed. This peak shows that only a 204 texture exists in specular direction on the sample.
Specular X-ray measurements on samples made from lower nabumetone concentrations do not show any crystallisation on or in the PMMA matrix which demonstrates the capability of PMMA to suppress crystallization.

4.4 Toluene as solvent

4.4.1 Films from spin coating

Nabumetone thin films were prepared from nabumetone/toluene solutions with different concentrations by using spin coating technique for deposition. Native silicon wafers and glass served as samples substrates.
Figure 4.21 shows the polarized optical microscope measurements for some chosen samples with varying concentration. The spin velocity was set to 30 rps. The sample made from the 100 mg/ml nabumetone solution reveals the formation of crystalline spherulites on the silicon substrate(Figure 4.20a). Those spherulites have a width of about 1 mm. Investigations of the whole surface by eye and microscope exhibit a film, which covers completely the silicon substrate.

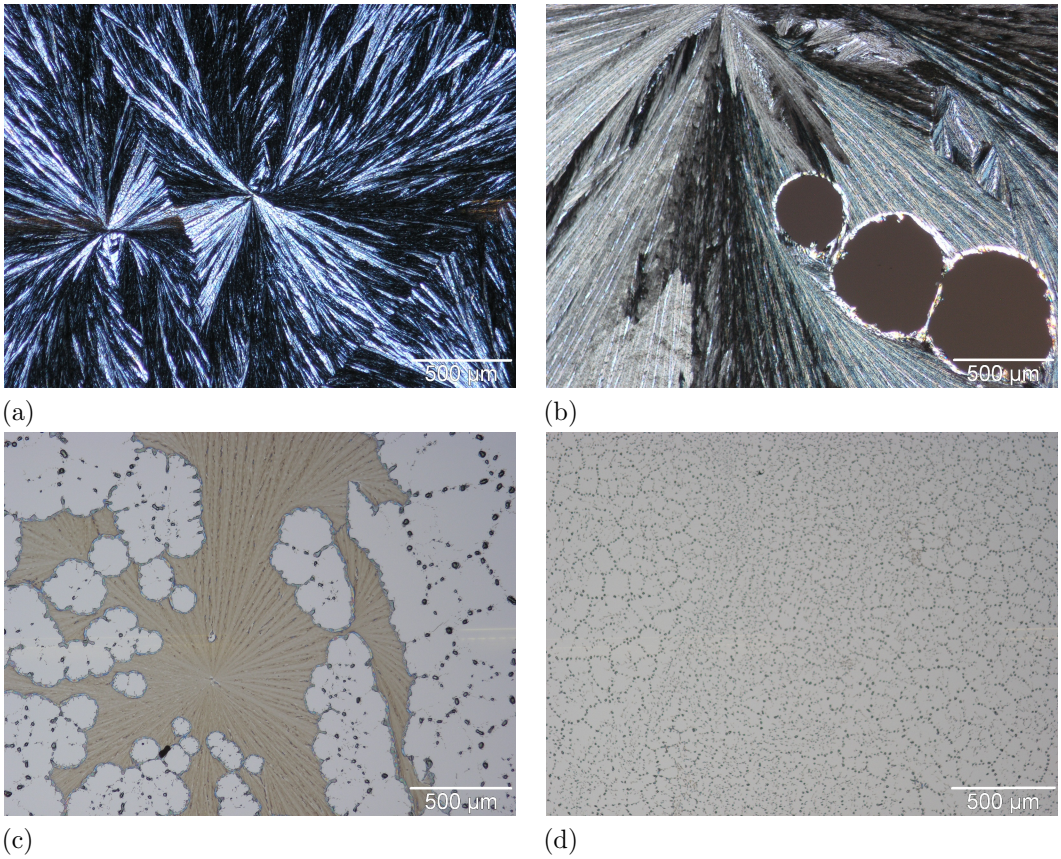

(a) (b)

(c) (d)

Figure 4.20: Images from optical microscope measurements of spin coated nabumetone/toluene films on native silicon with an amount of 50 μl and a spin velocity of 30 rps, The used nabumetone concentrations were: a): 100 mg/ml, b): 25 mg/ml, c): 12.5 mg/ml; d): 3.12 mg/ml.

The picture of the second sample (Figure 4.20b) made from a 25 mg/ml solution

reveals still a crystallisation in spherulites of nabumetone. Beside those spherulite formation dewetting layers appeared all over the substrate, with a width between 250 µm and 500 µm.
Using a 12.5 mg/ml nabumetone/toluene solution, so half of the second sample concentration, results in an increase of dewetting(Figure 4.20c). In comparison with the previous dewetting the width is smaller. Around those mounds/islands were formed with a size of a few micrometers. However, a spherulite still formed on the substrate but the typical shape was lost due to dewetting.
The fourth sample was prepared using a nabumetone concentration of 3.12 mg/ml. The optical micrograph (Figure 4.20d) reveals that the dewetting increased in a way that no spherulites can be observed. Moreover, only islands/mounds, which are randomly distributed over the surface, exist. Those islands have a very small size of a few micrometers.
The results from the specular X-ray diffraction measurements for various spin coated films are depicted in Figure 4.21. All data were collected in the range of 2Θ = 5-30°. The measurement on the sample from the 100 mg/ml solution exhibits one high intense peak located at 2Θ = 21.49°and some low intense peaks at 7.95°, 10.69°, 17.21°and 17.79°. The comparison of those peaks with the known peak position of various nabumetone forms reveal the stable polymorph 1, with a preferred 204 texture due to the peak located at 21.49°.

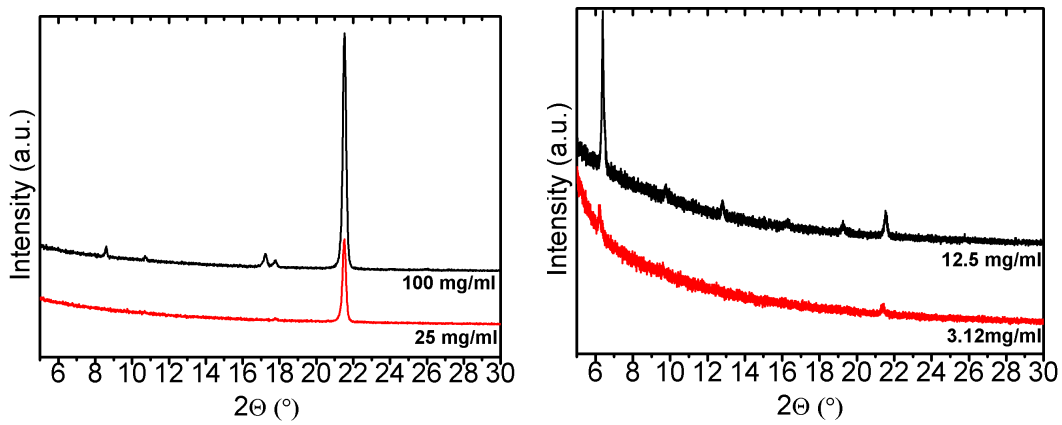

(a) (b)

Figure 4.21: Specular X-ray diffraction data of spin coated nabumetone/touene films on native silicon substrates from solution of a): 100 mg/ml and 25 mg/ml, b): 12.5 mg/ml and 3.12 mg/ml, Curves are shifted for clarity.

The X-ray pattern of the second sample, which was made from a 25 mg/ml solution, exhibits only one peak located at 21.5°, which indicates the (204) plane of polymorph 1 in specular direction on the substrate.

The sample prepared from the 12.5 mg/ml nabumetone/toluene solution shows some various peaks. The most intense peak is located at 6.51° and belongs to the (200) plane of the metastable polymorph 2. Furthermore, peaks can be observed belonging to higher orders of the 100 orientation of polymorph 2. Additionally the diffractogram reveals the 204 peak of polymorph 1, but with a lower intensity than the 200 peak. For a nabumetone concentration of 3.12 mg/ml the X-ray scan of the fourth sample reveals, compared with the previous results, only two low intense peaks. One is located at 6.51° and is a result of the polymorph 2 (200) pane. The other peak at 21.49° belongs again to the (204) peak of polymorph 1
The variation of the spin velocity did not change the polymorph selection, which means that only at high concentrations only polymorph 1 was observed, independently how fast the spin velocity was set.

Grazing incidence X-ray diffraction

To get additional information, Grazing incidence X-ray diffraction (GIXD) measurements were prepared at the Elettra Synchrotron. Figure 4.22 reveals an exemplarily GIXD result for a spin coated 25 rps spin coated film from a 100 mg/ml nabumetone/toluene solution together with calculated Bragg peaks (white cycles). The angle of incidence was set to 1.7°.
In specular direction, q_{xy} =0 $\mathring{A}^{-1}$, a few peaks can be observed, which are smeared due to large mosaicity. The most intense peak lies at the ring of the (204) plane. That peak is also the most intense peak in the specular scan (Figure 4.21) of the same sample. Also the low intense peak from the specular pattern can be observed. Moreover, various peaks are present in plane. All observed peaks beside the pink cycle, which describes the Bragg peak of the (1,1,1) plane from the silicon substrate, have their origins in polymorph 1. The calculated Bragg peaks fit very well to the experimental results.

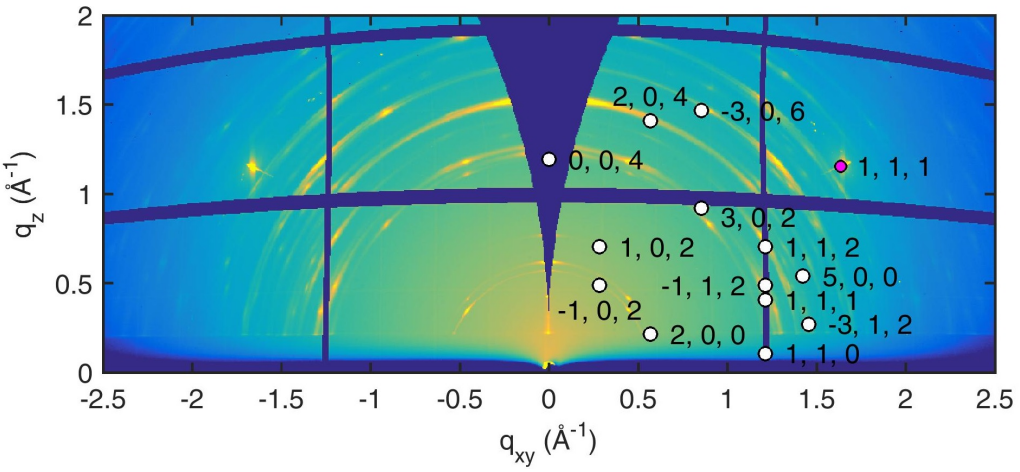

Figure 4.22: Results from GIXD measurements of a 100 mg/ml nabumetone/toluene film spin coated with 25 rps on native silcon, the white and pink cycles describe calculated position of Bragg peaks of nabumetone form 1.

4.4.2 Films from dip coating

Dip coated films were prepared from different nabumetone/toluene concentrations and with various withdraw speed. Figure 4.23 reveals light microscope images for samples prepared from a concentration of 50 mg/ml at two different withdraw velocities. The first figure 4.23a shows a sample produced at a withdraw velocity of 5 µm/s. The left side of the picture is the upper side of the sample, which comes out of the solution at first. The needles started to crystallize in every direction and very randomly. Areas of high nabumetone concentrations, dark regions can be observed. When the withdraw process continued, the right side of the picture, needles were formed, which had a certain growth direction. The needles grew downwards, due to the fact of withdrawing and reflowing of the nabumetone/toluene solution into the vessel. At lower sample regions this crystal growth continued. On the top of the directed needles also some dark high concentrated nabumetone areas can be observed. The width of the needles varies between a few µm and hundreds µm.
The second sample prepared with a withdraw velocity of 10 µm/s is shown in figure 4.23b. The right side is the upper area of the sample. It can be seen that at first needles crystallized in a certain direction, but with a lower concentration than on the lower (left) part of the sample. The needle density is for some region so high, that it is impossible to distinguish between individual needles. Thus, those rods of needles seem to be plates. Due to high concentrations of nabumetone dark islands can be observed on the needles. The needle width varies between a few µm and 1 mm.
Figure 4.23c depicts a sample prepared from a 150 mg/ml nabumetone/toluene

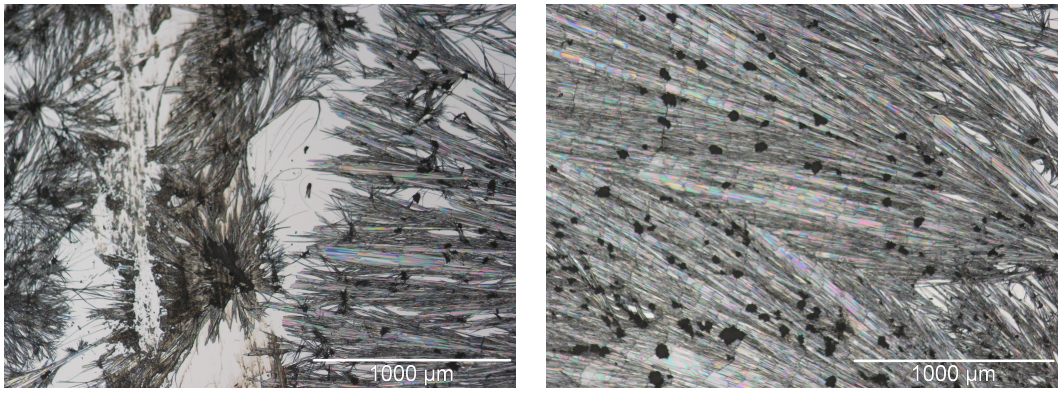

(a) (b)

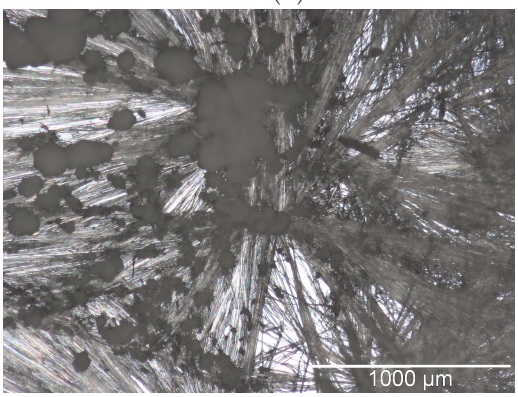

(c)

Figure 4.23: Images from optical microscope investigations of dip coated nabumetone/toluene films on native silicon and withdraw velocities of a): 5 µm/s and a concentration of 50 mg/ml with a withdraw direction from the left side, b): 10 µm/s and a concentration of 50 mg/ml with a withdraw direction from the right side, c) 4 µm/s, For all samples a concentration of 150 mg/ml was used.

solution with a withdraw velocity of 5 µm/s. A distinction of the upper and lower part of the sample is not possible, because the needles crystallized in every direction, without a preferred growth direction. On the top of the film large areas of high concentrated nabumetone were formed and appear as dark areas in the figure. Moreover, the needles did not only grow in 2 dimensions but also 3 dimensions and have width of about 1 mm.

The specular X-ray diffraction data of various dip coated nabumetone films are shown in Figure 4.24. Measurements were done by $\Theta/2\Theta$-scans in a region between 2Θ =5°- 25°. Figure 4.24a shows the results of films prepared from a 50 mg/ml nabumetone/toluene solution with two different withdraw velocities. The black curve is the pattern of the sample produced by a withdraw velocity of 5 µm/s and reveals various peaks over the whole scan rage. The most intense peaks are located at 17.2° and 21.49°. Comparing the measured peaks with peaks of known nabumetone

spectra reveals that all peaks have their origin in the stable polymorph 1. The appearing of so many peaks shows that the film behaves like a powder with only a slightly preferred orientation.
The red curve belongs to a sample prepared with a withdraw velocity of 10 µm/s. The X-ray pattern shows as many peaks as the result of the sample prepared at 5 µm/s. The strongest peaks are again those at 17.21° and 21.49°. The peaks clearly indicate that polymorph 1 exists on the sample. Also the powder like structure with a preferred orientation can be observed.

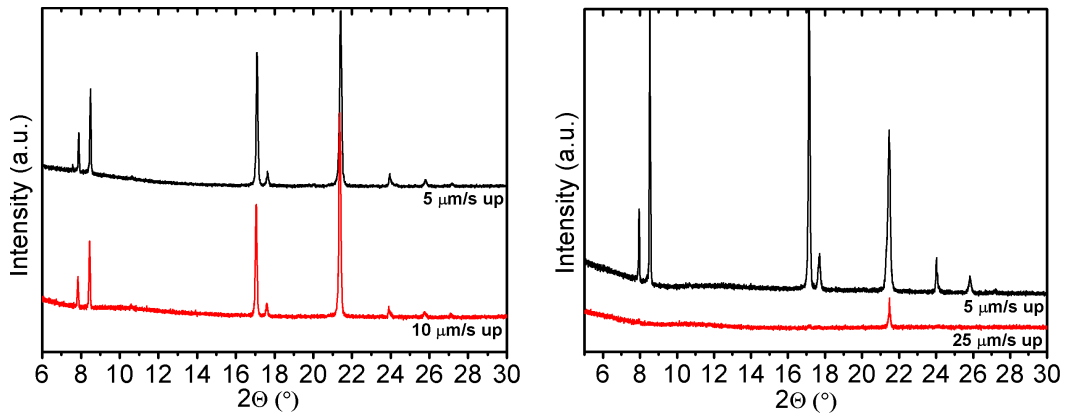

(a) (b)

Figure 4.24: Specular X-ray diffraction data of dip coated films from a): 50 mg/ml nabumetone/toluene solution with a withdraw velocity of 5 µm/s and 10 µm/s b): 150 mg/ml nabumetone/toluene solution with a withdraw velocity of 5 µm/s and 25 µm/s, Curves are shifted for clarity.

The figure 4.24b reveals XRD pattern from samples made from a 150 mg/ml solution at again two different withdraw velocities. The result of the sample prepared with a withdraw velocity of 5 µm/s (black curve) reveals many different peaks along the entire scan region. The most intense one are located at $2\Theta = 8.49°$ and 17.21°. This result exhibits that only polymorph 1 is present on the sample. The many visible peaks indicate a powder like behaviour of nabumetone. The comparison with an ideal powder reveal that a slight preferred orientation exists.
The second, red curve belongs to a dip coated film which was prepared with a withdraw velocity of 25 µm/s. In this pattern only one peak located at 21.5° is visible. That peak indicates a 204 texture of polymorph 1 on the sample.

4.4.3 Composite nabumetone-polystyrene

Polystyrene (PS) was used as a polymer matrix and as a crystallisation inhibitor similar to PMMA before. As there are some side effects by using different solvents nabumetone and PS were both dissolved in toluene. PS/toluene solutions were prepared with four different concentration between 7 wt.% and 0.15 wt.%. The preparation of various concentrations for the nabumetone/toluene solution started with 100 mg/ml and were halved as long until a concentration of 0.78 mg/ml were reached. Thus, eight different solutions were produced. For the preparation the two solutions were mixed together in a ratio of 1:1. The mention concentration refer to the initial concentrations before mixture.

Due to the great number of different samples only a few results of them are presented here,especially such for which strong differences were observed. The first sample series was prepared with 7 wt.% PS and different nabumetone concentrations and in the following figure selected samples are depicted (Figure 4.27). The sample prepared from a 100 mg/ml solution with PS reveals that the nabumetone crystallized on the surface in two different shapes. The large grain consists of needles, which formed a large spherulite. On the outside of the spherulite smaller plates can be obtained. In the background the colourful polystyrene is visible.

The second sample made from a solution of 50 mg/ml is depicted in figure 4.25b. It shows the formation of nabumetone elongated plates on a PS surface, which shows flower-like islands on a blue background. A few micrometers beside the plates some crystals were formed onto those islands.

Figure 4.25c exhibits a sample prepared from a 25 mg/ml solution and shows the formation of long dendrites on a blue PS surface. On some of those dendrites nabumetone crystals can be observed. The big black objects are dirt. In figure 4.25d islands are visible, which were formed on a blue/green PS substrate. It can not be distinguish if those islands are due to dirt or nabumetone.

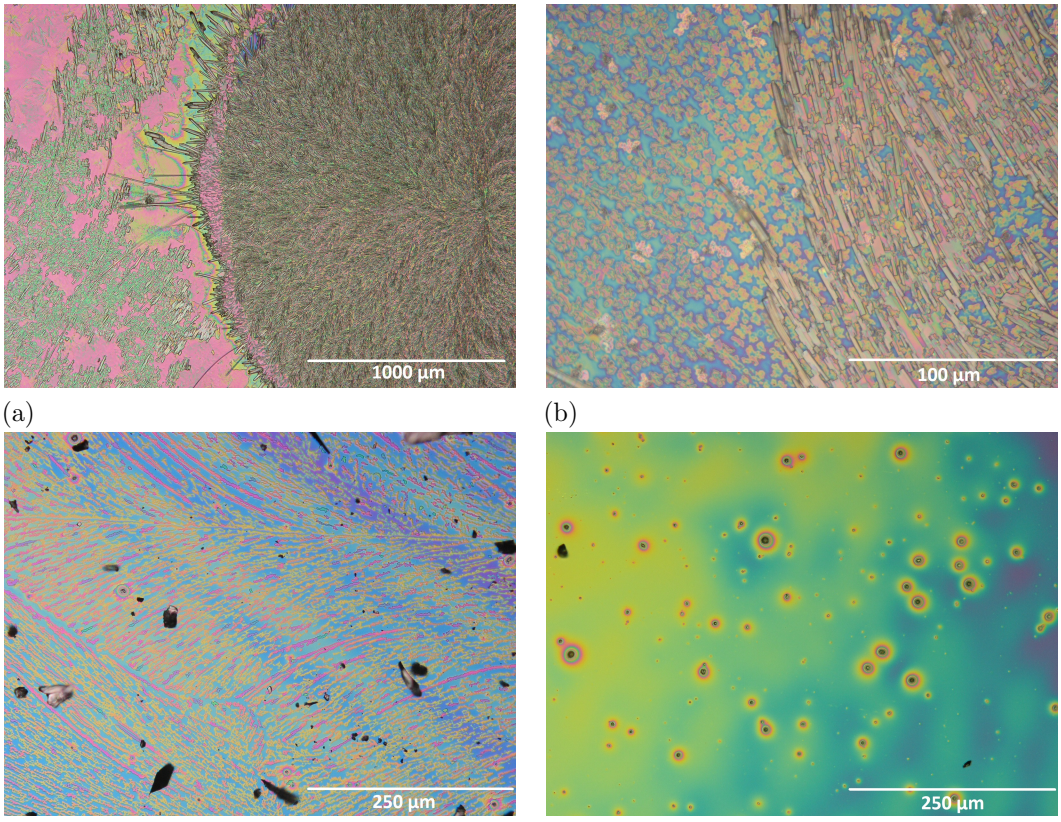

(a) (b)

(c) (d)

Figure 4.25: Optical micrographs of spin coated nabumetone/PS films on native silicon with a velocity of 30 rps, the concentration of PS was 7 wt.% and the used nabumetone/toluene solution were a): 100 mg/ml, b): 50 mg/ml, c):25 mg/ml; d): 12.5 mg/ml.

Specular X-ray scans were prepared in a region between $2\Theta = 5°$- $30°$ as this region provides the most important information. The results are depicted in Figure 4.26. The data from the first sample made from mixing of a 100 mg/ml solution with 7 wt.% PS reveals one intense sharp peak located at $2\Theta = 21.49°$ and a few broad peaks with a lower intensities at 6.51°, 9.76°, 13.21° and 16.38°. The comparison with known forms of nabumetone reveals that the intense peak results from the stable polymorph 1 and belongs to the (204) plane. The broad peaks has their origin in the metastable polymorph 2 (100) plane and belongs to the higher orders. The reason for the broadening of the peaks is the small crystal size in z-direction, perpendicular to substrate surface.

Scanning the second sample made from a 50 mg/ml nabumetone solution result again in a strong peak at 21.51°from polymorph 2. Moreover a weak peak is visible at 6.5°. This peak indicates the polymorph 2 [100] direction.

The XRD pattern of the sample prepared with a 25 mg/ml concentration has two visible peaks at 2Θ =21.51° and 28.4°. Those peaks indicate that only polymorph 1 is

present on the sample. Using the 12.5 mg/ml nabumetone for the sample preparation result in no crystallisation of nabumetone, which are visible in specular scanning directions which might have being expected from the optical microscope images.

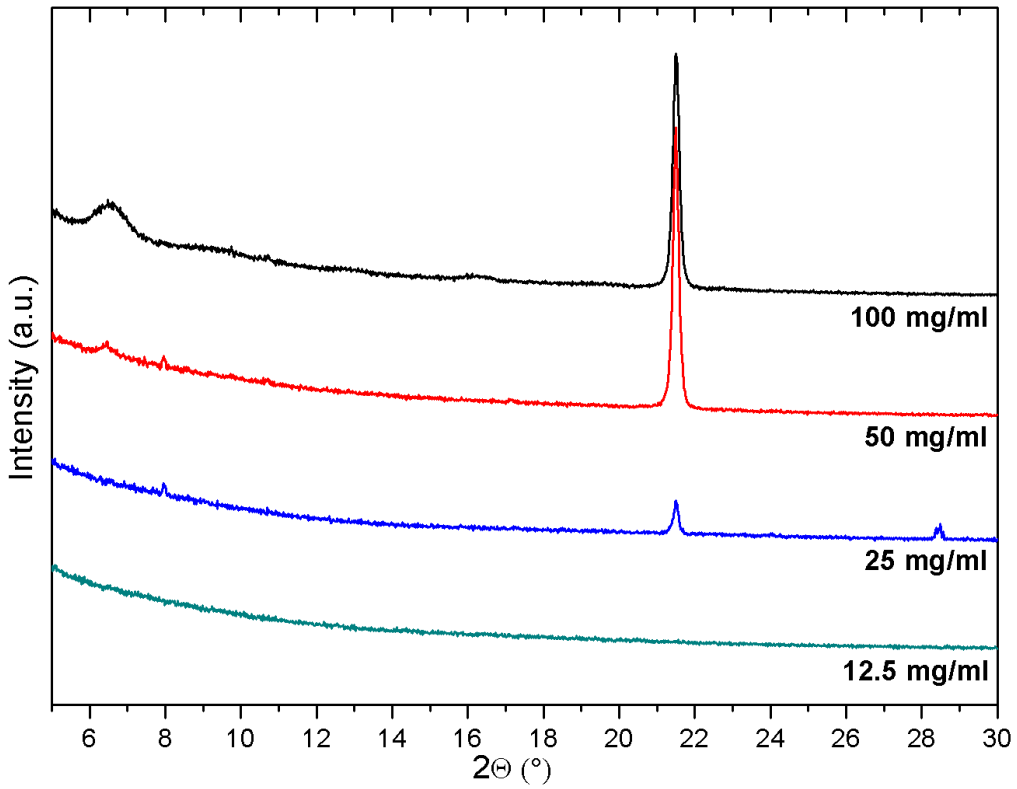

Figure 4.26: Specular X-ray diffraction scans of spin coated films prepared from mixing a 7 wt.% PS solution with different nabumetone concentrations, Curves are shifted for clarity.

Another series was prepared from mixing a 1.5 wt.% PS/toluene solution with different concentrations of nabumetone/toluene solutions. After mixing the new solution were spin coated with a spin velocity of 25 rps on native silicon substrates. In the following figure selected optical microscope images and a photograph of a whole sample are depicted.

Figure 4.27a depicts a microscope picture of the sample made from a 100 mg/ml nabumetone solution. The nabumetone formed a pink shining grain on the surface. That colourful grain indicates, that PS built a polymer matrix with nabumetone in it. At the surface of that small needles can be observed and at the grain boundaries long needles crystallized. The width of the needles varies between a few µm and hundreds of µm. Moreover, some small islands formed on a very thin film of PS.

The photograph of the film from the 50 mg/ml solution on a 2 cm x 2 cm native silicon wafer (Figure 4.27b) shows on one hand spherulites, dark reflecting areas, on

the other hand large grey areas in between. Thus, pictures with optical microscope were taken separately in those two areas using a polariser, to visualize crystals. Figure 4.27c reveals the taken micrograph of the grey area. The nabumetone crystallized in small plates with a size of a few µm. The plates appear not so bright, which means that they lies under the brighter ones. The taken images of the spherulite center is depicted in figure 4.27d. It reveals the crystal growth of nabumetone needles in every direction.

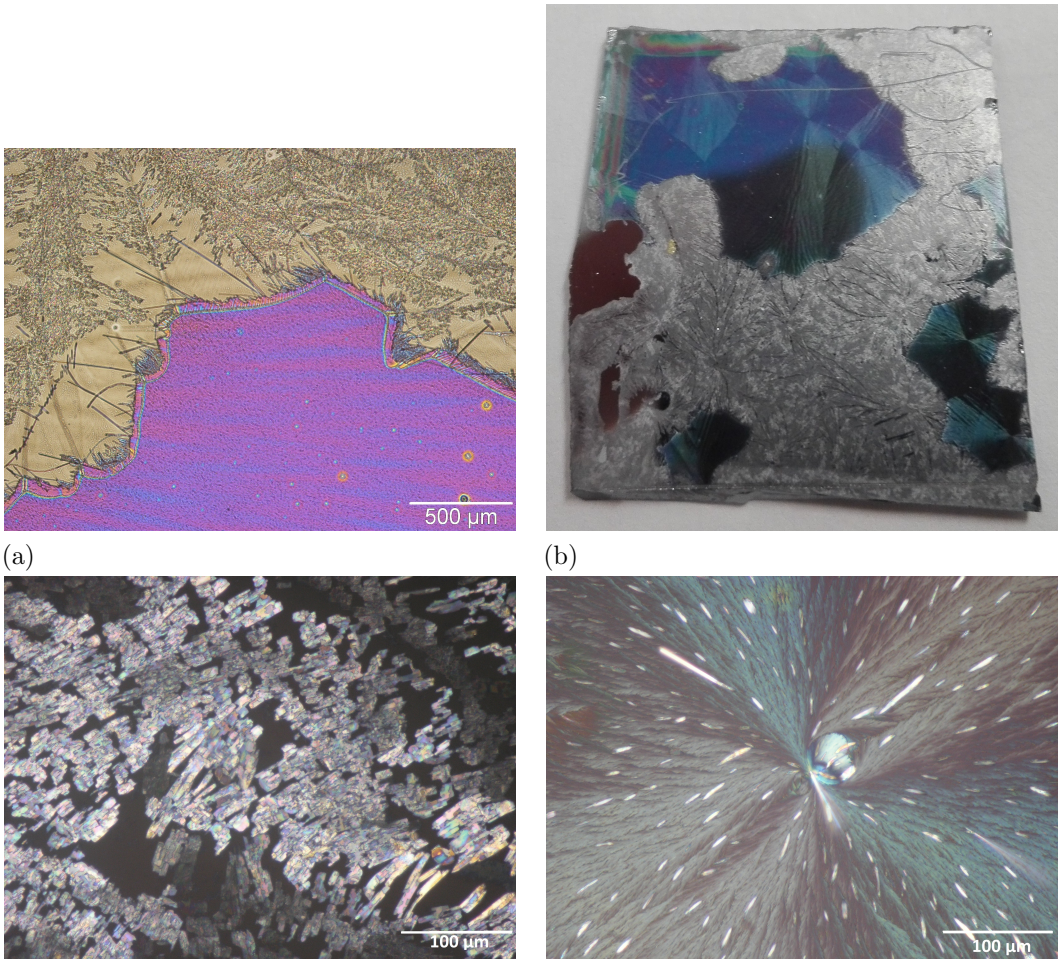

(a) (b) (c) (d)

Figure 4.27: Optical micrographs of spin coated nabumetone/PS films on native silicon with a velocity of 25 rps, The concentration of PS was 1.5 wt.% the used nabumetone/toluene solutions were a): 100 mg/ml, b)c)d): 50 mg/ml, same sample but different areas, b) overview picture of the 50 mg/ml sample, c) grey area from the overview, d) spherlulite from the overview.

Specular scans of the nabumetone/PS films were made in a range of $2\Theta = 5°$-$30°$ and are depicted in Figure 4.28. In the left figure 4.28a taken scans for different nabumetone concentrations can be observed.

The XRD pattern for the sample prepared from a 100 mg/ml solution reveals various peaks with the strongest located at $2\Theta = 6.5°$ and 9.8°. Lower intense peaks are distributed over the whole scan range. Comparing the XRD pattern with known nabumetone polymorphs, shows that both polymorphs are present on the substrate. The most intense peaks are a result of higher orders of the metastable polymorph 2 (100) plane. Peaks located at 7.95° and 21.51° are the diffractions of the polymorph 1 planes (10-2) and (204).
Scanning the second sample, red curve, results in a pattern with one intense peak at 21.51° and two weak peaks at 7.95° and 17.21°. All three peaks belongs to polymorph 1 planes. The strongest one indicates a (204) texture on the substrate.
Using the 25 mg/ml nabumetone/toluene solution for preparing the third sample views only one peak at 28.39°. This peak comes from the silicon substrate. Thus no crystallisation of nabumetone in specular direction can be observed.

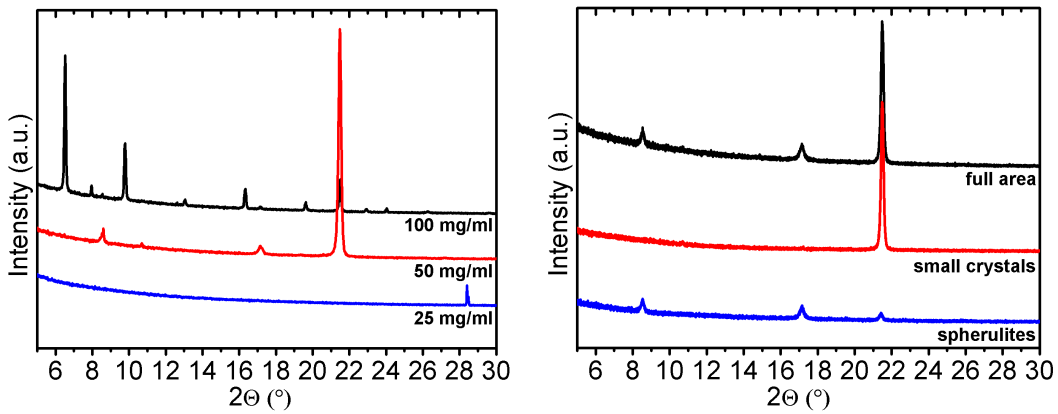

(a) (b)

Figure 4.28: Specular X-ray diffraction scans of spin coated films prepared from mixing a 1.5 wt.% PS solution with a): different nabumetone concentration, b) scans of different areas of the sample prepared from a 50 mg/ml nabumetone solution, Curves are shifted for clarity.

The right figure 4.28b shows XRD pattern of always the same sample, which was prepared from the 50 mg/ml solution. The black curve reveals the scan over the full area, with both spherulites and the grey area knowing from the figure 4.27b. The red curve is the result from the grey area, which was formed by small crystals. The scan reveals only one peak located at 21.51°. Thus, the small crystals have a 204 texture of stable polymorph 1.
The scan of the spherulites is depicted in the blue curve. It shows three peaks, which are located at $2\Theta = 7.95°$, 17.21° and 21.51°. All peaks are a result of polymorph 1 and describe the diffraction from (10-2), (110) and (204) planes.

Producing further sample series under same conditions and the same concentrations as for the 1.5 wt.% PS solution, showed at first polymorph 2 was formed. After some weeks form 2 started to recrystallize to polymorph 1. The speed how fast that recrystallisation took place depended on the environment conditions.

Grazing incidence X-ray diffraction

Grazing incidence X-ray diffraction (GIXD) measurements were done for the sample prepared from mixing a 100 mg/ml nabumetone/toluene solution with 7 wt.% PS/toluene and then spin coating on native silicon substrate. The GIXD map is shown in Figure 4.29 with calculated Bragg peaks. The red cycles describe peaks from polymorph 2, the white ones polymorph 1 and the pink the (1,1,1) reflection of the silicon substrate.

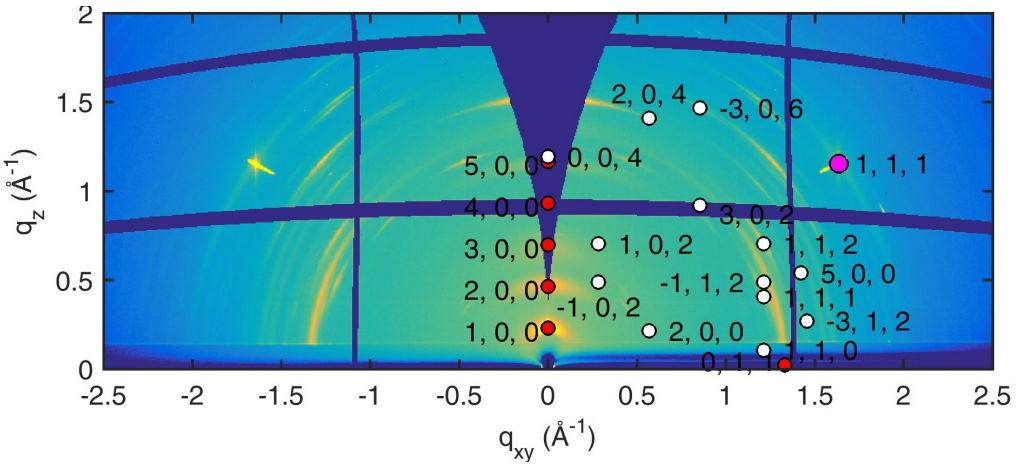

Figure 4.29: GIXD map from measurements of nabumetone/PS film spin coated at 25 rps, the nabumetone solution was 100 mg/ml and the PS concentration 7 wt.%, The cycles describes calculated Bragg peaks of polymorph 1(white cycles) and 2(red cycles).

In specular direction, $q_{xy} = 0$ $\mathring{A}^{-1}$, broad peaks from the 100 texture of polymorph 2 can be observed. The peak broadening is a result of small crystal repeating units of polymorph 2 nabumetone. An other peak located at $q_{xy} = 0$ $\mathring{A}^{-1}$ and $q_z = 1.5$ $\mathring{A}^{-1}$ belongs to the (204) plane of polymoprh 1. That result for GIXD in specular direction fits with the measured XRD pattern for the same sample (Figure 4.26). In plane the GIXD map only shows peaks from polymorph 1.

Chapter 5

Discussion

Nabumetone is a small molecule of low polarity. This low polarity is reflected in the very high solubility in Tetrahydrofuran (THF) and toluene while for ethanol the dissolution is much less. From this behaviour high concentrated solutions of 150 mg/ml in either toluene and THF could be easily prepared. In ethanol 20 mg/ml was the maximal used values, as above this concentration undissolved material could be identified. It should be stated, that an exact evaluation of the maximum solubility was not performed. It might be that the solubility in THF and toluene can exceed those values. Nevertheless, for the studies here this solution remained stable without any deviating behaviour over time, so that a lot of experiments could be repeated without using fresh solutions. Having this stable solution enabled using spin coating, drop casting and dip coating to evaluate the impact on the film forming properties as well as on the polymorph formation.

Drop casting is a very simple method to coat a surface. In course of the experiments during this work it followed that the solute content, the drop size, evaporation rate and the surface besides the solvent have decisive impact on the crystal morphology but also on the polymorph. Starting exemplarily with a large concentration of nabumetone in ethanol it can be seen, that crystals form into large needles sitting at the surface. While the experiment was conducted at a substrate the needles did not show any preferred orientation. This suggests that the crystallization already started in the drop (bulk solution) where an arbitrary direction was initiated. On the solvent removal most of those needles just fall onto the substrate forming the apparent morphology in Figure 4.1. Hereby the substrate seems to be of minor importance so that the behaviour is governed by the high level of supersaturation quickly reached in the solution with ethanol. The reduction of the concentration changed this behaviour drastically and the previous 3-dimensional growth is exchanged a film formation, i.e. a more 2-dimensional type of structure. This can be understood again by the level

of saturation. Hereby, the initially low nabumetone content prevents the system from crystallization. During the evaporation the drop size and height reduces which coincide with an increase in saturation. As a result, the crystallization is now taking place in a more two-dimensional confined space which results in the morphology observed in Figure 4.4.

Changing the substrate to a PS surface a more two-dimensional growth with elongated plate like structures formed (Figure 4.4). This shows that other than the silicon oxide surfaces the solid–liquid interface impacts the crystal formation. This is also reflected by the crystallographic texture which was much more defined, with only one contact plane being present within one sample.

The introduction of a unidirectional process route, i.e. dip coating, resulted in the needles of nabumetone being aligned along the withdraw direction(Figure 4.12). This results from the liquid–air interface being aligned and dragged along the surface. At this interface the level of saturation exceeds the maximum which promotes crystal growth aligned with respect to the evaporation line. Using very high concentrations, again crystallization takes place, but as the supersaturation is too high the evaporation line does not impact significantly the crystal growth direction; arbitrary crystal direction are observed. The change in the withdraw velocity results in the film morphology changing, whereby the slow velocity in general allows for a single crystal growing much longer. In the case of the faster, there the withdraw direction impacts much more the final direction, as side branched crystals cancel by geometrical constrains.

To get a better control over the film thickness and the evaporation rate the spin coating technique was applied, since the surface-liquid-air interface can be adjusted to be very narrow. By changing the spin velocity, the film thickness could be varied between a few µm down to nm regions. At one hand, the evaporation rate increased by setting higher spin velocities and on the other hand more material was removed from the substrates by centrifugal forces. In the case of using ethanol, small islands of nabumetone crystallized onto the surfaces and built a rough film observed in Figure 4.6. Those islands became smaller by adjusting a higher spin velocity. A similar behaviour was observed by varying the nabumetone concentrations. Here, the crystal size of the formed islands could be changed by those different concentrations. Higher concentrations resulted in larger crystals.

Further experiments with toluene and THF as solvents revealed mostly due to higher concentrations, a different behaviour. The usage of solutions at a high level (100mg/ml) resulted in the formation of a few large spherulites. Hereby, nabumetone crystallized in long needles, starting at one common point, in every direction on the

substrate. Thus, films, which covers the entire area of the substrates were possible. Nevertheless, those films had a high roughness. At high concentrations the level of supersaturation reaches very fast maybe even leaving an initial amorphous state. Consequently, the centre of the spherulites were induced by impurities on the sample surface. In the case of those samples only a small number of such defects were present on the substrate surfaces. The lowering of the nabumetone concentration effected beside the spherulites formation a dewetting. Thus, the films got more inhomogeneous. Around the dewetting small islands crystallized. A further decrease in concentration down to regions of ethanol showed a similar behaviour known from ethanol. Here, only independent islands crystallized on the substrates (Figure 4.16, Figure 4.20).

Composite film with nabumetone and PMMA were prepared to inhibit the crystallization and to introduce a matrix(Figure 4.18). In the PMMA matrix nabumetone should crystallize in the free space between the PMMA chains. Starting with a high concentration, the nabumetone formed plates on the PMMA surfaces while, those plates disappeared at lower concentration, since the nabumetone sits between the long PMMA strains. Whereas the nabumetone at high concentrations had filled up those spaces in the matrix. Consequently, the rest of nabumetone had to crystallize onto the PMMA surface. Furthermore, composite films with PS were prepared to investigate the behaviour in a second polymer matrix (Figure 4.27). Moreover, the influence on varying the polymer concentration was inspected. At high concentrations again, the space between the matrix was filled completely with nabumetone and thus the remaining nabumetone crystallized on the polymer surface. However, the investigations showed, that here two different morphologies appeared. Beside small plates a small number of spherulites were formed. Those spherulites were only formed at the highest used concentration, since the crystallization happened at defects, which are rarely, on the nabumetone/PS composite surface. Smaller concentrations resulted at first in crystallisation of small plates. Further dilution showed that no crystals were formed at the PS surface. Therefore, the residual nabumetone had to sit in between the PS-chains.

Table 5.1: Comparison of the different results for the nabumetone films prepared from different processes and solutions

Solution/polymer matrix	Thin film technique	Morphology	Dominant phase
Ethanol			
	Drop casting	Needles	Form 1
	Spin coating	Mounds	Form 2, Form 3
	Dip coating	Needles	Form 1
THF			
High concentrations	Spin coating	Spherulite	Form 1
Low concentrations	Spin coating	Mounds	Form 2
PMMA	Spin coating	Spherulites	Form 1, Form 2
Toluene			
High concentrations	Spin coating	Spherulites	Form 1
Low concentration	Spin coating	Mounds	Form 2
	Dip coating	Needles	Form 1
Polystyrene	Spin coating	Spherulites	Form 1

Polymorphism is the behaviour of a material to exist with the same chemical structure in different crystal forms. Those forms can have an impact on different properties, e.g. thermodynamics, chemical stability, optical/electric properties and dissolution properties, which effects itself the bioavailability. Stable polymorphic phases(bulk phase) are in principle less soluble than metastable phases. Consequently, polymorphism and the understanding of their selection is important to define new drug therapies or improve existing formulations.

The polymorphism of nabumetone was described in literature to consist of two different polymorphs. Polymorph 1 is here described as the thermodynamically stable one. It possesses a monoclinic crystal structure with eight nabumetone molecules within the unit cell. The melting temperature of polymorph 1 lies at about 80°C. The density is $\rho = 1.26\ g/cm^{-3}$. Polymorph 2, the thermodynamically less stable form, also crystallizes in a monoclinic structure, but with only 4 molecules per unit cell and has a melting temperature at about 65°C. The density is a bit degraded to 1.21 g/cm^{-3}. Both, the melting temperature and the density of polymorph 2, are a hint without an experimental proof, that polymorph 2 is the thermodynamically less stable phase. Nevertheless, stability tests were done to get more information about the recrystallisation process. Here the same sample was scanned one week and one month after processing. The results revealed that the pure polymorph 2 100 texture was completely transformed after one month into a polymorph 1 204 texture. Furthermore, two heating experiments were done to improve that behaviour observed in Figure 4.15. Polymorph 2 recrystallized at the first experiment to stable polymorph by 1 reaching 65°C. A direct recrystallisation back to polymorph 2 was

not observed but it was possible to get it by melting first polymorph 1 and quench the sample afterwards. Through this process polymorph 2 crystallized on the samples. Those results reveal a monotropic behaviour of nabumetone polymorphism.

Specular X-ray diffraction (XRD) scans from drop casted films, independently on the used solvents, showed that polymorph 1 was dominant at high concentration without a preferred Orientation(Figure 4.2). Whereas the lowering of concentrations resulted in the formation of polymorph 2 with a 100 texture. The usage of a cover to lower the evaporation rate (Figure 4.3) effected the polymorph selection in a way, that only polymorph 1 crystallized. Moreover, a change in texture happened; the (10-2) and the (204) planes were observed. Drop casting itself is a very slow process. Thus, the prepared films have plenty of time to crystallize. A second slow technique is dip coating. Here, the X-ray scans revealed only the formation of polymorph 1 with mainly slight preferred orientations. Variations in withdraw velocity had a modest influence on the texture selections.

Does faster speed in preparation process result in polymorph 2? To check this hypothesis, the spin coating method was used due to the fast evaporation rates. High concentrated solution from THF and toluene showed at first another behaviour than expected(Figure 4.17,Figure 4.21). Here, only polymorph 1 was formed using either solvents. Moreover, always a 204 texture was observed in specular direction. The observed spherulites consisted thus only of polymorph 1 but having three different orientations in specular directions. The needles do not crystallize simple in one direction but also are twisted along their growth directions. The appearing of dewetting on the samples at lower concentrations exhibited that polymorph 1 started to disappear and polymorph 2 was formed with a 100 texture. XRD scans of the composition nabumetone/PMMA revealed (Figure 4.19) the formation of both polymorphs at high nabumetone concentrations. Polymorph 1 had always a 204 texture with large crystal repeating units in z-direction perpendicular to the sample surface, indicated by a sharp peak, while the polymorph 2 peaks, again in a 100 texture, were very broad, which indicates the presence of crystals of low height. At lower concentrations no crystallinity could be observed. Thus, the nabumetone molecules, which sit in between of the PMMA matrix stayed amorphous and formed likely a solid states solution with PMMA. A similar behaviour was observed by using a 7 wt.% PS. Here, again both polymorphs were observed with the same textures and shape of the peaks(Figure 4.26). Decreasing the nabumetone concentrations resulted in amorphous solid states solutions. At a PS concentration of 1.5 wt.% the

polymorph 2 peaks got narrower. Thus, the crystals got larger. Moreover, grazing incidence X-ray diffraction (GIXD) measurements revealed in Figure 4.22 confirmed those results from XRD. Additionally, differences in the orientations of spherulites and plates of polymorph 1 exist in figure 4.28b. While spherulites have due to their twist different orientations, the plates only show a (204) texture.

Using ethanol as solvent for spin coating resulted in the formation of polymorph 2 independently of various spin velocities $\leq$ 10 rps (Figure 4.7. The only observed orientation was a 100 texture with appertaining higher diffraction orders. Due to low spin forces the polymorph 1 204 texture appeared at slow spin velocities. Variations in nabumetone concentrations revealed the same behaviour in the XRD pattern in Figure 4.8. High concentrations effected the formation of a purer polymorph 2 selection. Remarkable in the pattern was the very low intensities of the (400) peak compared to the (500) peak of polymorph 2. That effect can be explained by the small change of the electron density at the (400) plane. Closer investigation on spin coated nabumetone/ethanol films revealed the formation of additional peaks near to the (200), (400) and (600) peaks of polymorph 2. Those peaks are unexplainable by form 1 or form 2 but can be described by a new polymorphic form 3. Since no pure polymorph 3 was produced the question was now, how their amount could be influenced. The simple variation of spin velocities worked in a dissatisfied way. Especially, to get only polymorph 2 was difficult. Form 2 became more dominant by increasing the spin velocities, but form 3 had still even at 70 rps the same intensity as form 2. Higher velocities resulted in thinner films. To gain further changes dynamical spin coated (DSC) was applied. Hereby, the solution was deposited on the sample after starting the spin coater whereby, more material washed away from the substrate due to centrifugal effects and thinner films were produced at the same velocities compared to the normal spin technique. Those experiments lead to a better but not perfect selection of form 2 or form 3. Here polymorph 2 was more likely formed by applying higher spin velocities. A big disadvantage of DSC was the relative high loss of material during the processing. Further adjustments will be needed to get only the new form. GIXD measurements showed in Figure 4.11 that mainly a 100 texture was present on the substrate. The additional peaks could not be observed due to the double peaks were to narrow thus only one big peak was detected by the detector.

Comparing the XRD results of spin coated films from ethanol, toluene and THF with the corresponding micrographs revealed that polymorph 2 formed small islands or plates. The shape of the unknown form 3 could not be distinguished from the shape of polymorph 2 but micro Raman spectroscopy might enables such an identification.

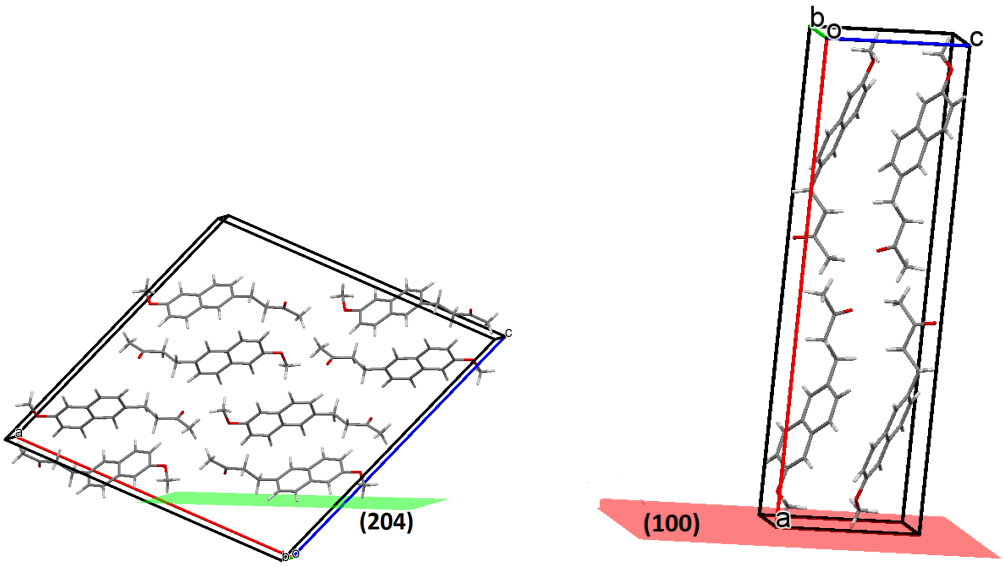

(a) (b)

Figure 5.1: Observed textures of nabumetone a): polymorph 1 (204) plane and b): polymorph 2 (100) plane

How can the polymorph selection be explained? It was shown that for slow processing, drop casting and dip coating, mainly bulk phase was formed, whereby the (204) plane were found most often even when a powder like structure was observed. The (204) plane is described by molecules "lying" on the sample substrates, which can be seen in Figure 5.1. Whereas, faster processing result for low concentrations in polymorph 2 with a 100 texture. Here, the molecules now stay on the substrate.

This behaviour can be explained by the Ostwald rule of stages. The rule describes that during the nucleation stage the metastable phase, here polymorph 2, are more probable to form. During the growth, the initial nuclei can transit into a more stable phase (polymorph 1). This is only possible, if enough time is available that low energetic (typically stable phase) forms can be formed.[55],[24],[56] The results show, that the Ostwald rule of stages very well explains the behaviour observed at thin films prepared from nabumetone/ethanol solutions.

However, within toluene and THF from high initial solution concentration spin coating resulted always in polymorph 1.These initial solutions might contain already polymorph 1 nuclei or crystals where heterogeneous nucleation taking place and the nuclei grow in the same structure of the mature crystal (Figure 5.2b). Another point is that high concentrations means that the level of supersaturation is achieved very fast. As a result, homogeneous nucleation happened at the liquid-vapour interface

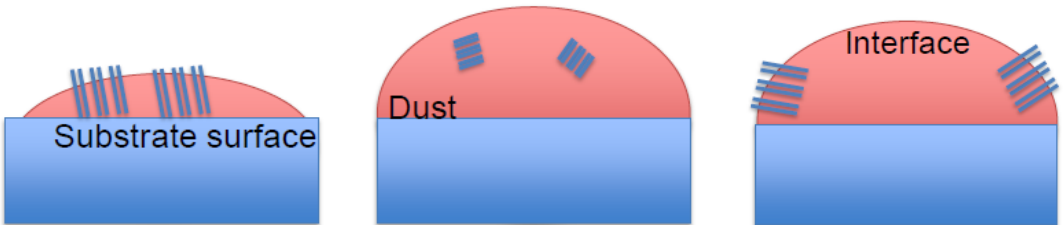

Figure 5.2: Three possibilities of nucleation in nabumetone thin films, a): heterogeneous nucleation at surface b): heterogeneous nucleation on dust, c) homogeneous nucleation due to supersaturation at liquid vapour interface

(Figure 5.2c), since the evaporation rate at the biggest curvature of the liquid drop is very high. Whereas, at low concentrations the liquid films are flatter than those of initial high concentrations and thus a stronger surface interaction is induced. The molecules can now build a confinement with the surface(5.2a). Hereby, the molecules form a 100 texture of polymorph 2. The surface itself is important for that heterogeneous nucleation but does not stabilize polymorph 2 and as a consequent the molecules "fall down" and recrystallize to polymorph 1 mainly in a 204 texture. Wetting-dewetting, seen by toluene and THF solution, might causes an additional confinement and surface interactions.

Chapter 6

Conclusion

The understanding of polymorphic selection in pharmaceutical drugs is crucial in obtaining new drug formulation. Beside the ingestion of tablets or liquids, the use of laminates and plasters get into the focus of investigation in the last years. Thus, thin films became important.

In the case of nabumetone different methods and solvents were applied to form thin films. It was shown that a proper selection of concentration and processing impact the selection of polymorphs in a way that both known forms and a new form were observed. The application of specular X-ray diffraction (XRD), grazing incidence X-ray diffraction (GIXD) measurements were powerful techniques to determine these forms of nabumetone.

Beginning with drop casted films from ethanol solutions the stable polymorph 1 was formed, beside low concentrations of the metastable form 2. Varying the evaporation rates results in a morphology change. Due to the low evaporation rate only form 1 was formed. Similar results were got by dip coating, where mainly polymorph 1 was formed on the substrates independently if glass or silicon were used. Furthermore, a change in the solvent also had no effect on the polymorph selection. Thus, it can be concluded, that slow evaporation rates result only in polymorph 1, while spin coating showed the opportunity of forming polymorph 2, due to the very high evaporation rates. Especially at ethanol solution nabumetone forms polymorph 2 by standing molecules on the substrates. Furthermore, a new polymorphic phase was observed. This new form revealed peaks in the XRD pattern and GIXD maps which were unexplainable by polymorph 1 or polymorph 2. Therefore, further investigations are needed to determine the shape of the new form. Using very high concentration of nabumetone in toluene and THF solution resulted in formation of polymorph 1. However, by decreasing the nabumetone concentrations polymorph 2 started to form, by the appearance of de-wetting layers. Unfortunately, this form 2 started after some

time to recrystallize to polymorph 1. Polymorph 1 crystals occurred mostly as long needles or plates, whereas form 2 crystals formed small islands, which are randomly distributed over the substrate surfaces.
Further controlled variation was achieved by varying the substrate environment using polymer matrices. Here, at low nabumetone concentrations now crystallinity could be observed. Whereas, the nabumetone molecules started to crystallize by forming both polymorphs onto the polymer surfaces when the concentration was high enough and all space between the polymer chains was filled up, whereby the form 2 crystals were very thin.
To summarize the results, a selection of both polymorphs is possible by using the right concentration and processing. Additionally, polymorph 2 needs the substrate to form, but the surface does not stabilize this form and a recrystallisation takes place after time which means it shelf life time, i.e. the time allowed to use is limited.

List of Figures

List of Tables

Bibliography

[1] J. Bernstein, *Journal of Physics D: Applied Physics* **1993**, *26*, B66.

[2] M. R. Caira in *Design of Organic Solids*, Springer, **1998**, pp. 163–208.

[3] R. J. Davey, S. L. M. Schroeder, J. H. ter Horst, *Angewandte Chemie International Edition* **2013**, *52*, 2166–2179.

[4] C. Röthel, H. M. A. Ehmann, R. Baumgartner, D. Reischl, O. Werzer, *CrystEngComm* **2016**, *18*, 588–595.

[5] J. De Yoreo, S. Whitelam, *MRS Bulletin* **2016**, *41*, 357–360.

[6] S. Karthika, T. K. Radhakrishnan, P. Kalaichelvi, *Crystal Growth & Design* **2016**, *16*, 6663–6681.

[7] J. Anwar, D. Zahn, *Angewandte Chemie International Edition* **2011**, *50*, 1996–2013.

[8] D W Oxtoby, *Journal of Physics: Condensed Matter* **1992**, *4*, 7627.

[9] D. Turnbull, *The Journal of Chemical Physics* **1950**, *18*, 198–203.

[10] R. Sear, *MRS Bulletin* **2016**, *41*, 363–368.

[11] M. L. Whittaker, P. M. Dove, D. Joester, *MRS Bulletin* **2016**, *41*, 388–392.

[12] U. Thiele, M. Mertig, W. Pompe, *Physical review letters* **1998**, *80*, 2869.

[13] J. Russo, H. Tanaka, *MRS Bulletin* **2016**, *41*, 369–374.

[14] A. Mersmann, M. Kind, J. Stichlmair, *Thermische Verfahrenstechnik: Grundlagen und Methoden* **2005**, 413–482.

[15] C. Weißmantel, C. Hamann, *Grundlagen der Festkörperphysik*, Johann Ambrosius Barth Verlag, **1995**.

[16] C. Kittel, J. M. Gress, A. Lessard, *Einführung in die Festkörperphysik*, *Vol. 14*, Oldenbourg München, **1969**.

[17] B. Wedl, R. Resel, G. Leising, B. Kunert, I. Salzmann, M. Oehzelt, N. Koch, A. Vollmer, S. Duhm, O. Werzer, G. Gbabode, M. Sferrazza, Y. Geerts, *RSC Advances* **2012**, *2*, 4404.

[18] D. Singhal, *Advanced Drug Delivery Reviews* **2004**, *56*, 335–347.

[19] J. Bauer, S. Spanton, R. Henry, J. Quick, W. Dziki, W. Porter, J. Morris, *Pharmaceutical Research* **2001**, *18*, 859–866.

[20] L. Huang, *Advanced Drug Delivery Reviews* **2004**, *56*, 321–334.

[21] J. D. Dunitz, J. Bernstein, *Accounts of chemical research* **1995**, *28*, 193–200.

[22] A. O. F. Jones, B. Chattopadhyay, Y. H. Geerts, R. Resel, *Advanced Functional Materials* **2016**, *26*, 2233–2255.

[23] H. M. A. Ehmann, O. Werzer, *Crystal Growth & Design* **2014**, *14*, 3680–3684.

[24] J. C. Burley, M. J. Duer, R. S. Stein, R. M. Vrcelj, *European Journal of Pharmaceutical Sciences* **2007**, *31*, 271–276.

[25] D. Reischl, C. Röthel, P. Christian, E. Roblegg, H. M. A. Ehmann, I. Salzmann, O. Werzer, *Crystal Growth & Design* **2015**, *15*, 4687–4693.

[26] P. Christian, C. Röthel, M. Tazreiter, A. Zimmer, I. Salzmann, R. Resel, O. Werzer, *Crystal Growth & Design* **2016**, *16*, 2771–2778.

[27] A. D. Bond, R. Boese, G. R. Desiraju, *Angewandte Chemie International Edition* **2007**, *46*, 618–622.

[28] L. E. Alexander, *X-Ray Diffraction Methods in Polymer Science*, Robert E. Krieger Publishing Company, **1979**.

[29] M. Birkholz, *Thin film analysis by X-ray scattering*, John Wiley & Sons, **2006**.

[30] S. K. Park, T. N. Jackson, J. E. Anthony, D. A. Mourey, *Applied Physics Letters* **2007**, *91*, 063514.

[31] J. Park, S. Lee, H. H. Lee, *Organic Electronics* **2006**, *7*, 256–260.

[32] D. Bornside, C. Macosko, L. Scriven, *Journal of imaging technology* **1987**, *13*, 122–130.

[33] D. B. Hall, P. Underhill, J. M. Torkelson, *Polymer Engineering & Science* **1998**, *38*, 2039–2045.

[34] L. E. Scriven, *MRS Proceedings* **1988**, *121*, 717.

[35] D. Grosso, *Journal of Materials Chemistry* **2011**, *21*, 17033–17038.

[36] R. A. Carlton in *Pharmaceutical microscopy*, Springer, **2011**, pp. 7–64.

[37] L. Whittig, W. Allardice, *Methods of Soil Analysis: Part 1—Physical and Mineralogical Methods* **1986**, 331–362.

[38] S. K. Sinha, E. B. Sirota, S. Garoff, H. B. Stanley, *Phys. Rev. B* **1988**, *38*, 2297–2311.

[39] A. Afanas' ev, M. Melkonyan, *Acta Crystallographica Section A: Foundations of Crystallography* **1983**, *39*, 207–210.

[40] K. Kjaer, *Physica B: Condensed Matter* **1994**, *198*, 100–109.

[41] S. Stepanov, *3rd Autumn School on X-ray Scattering from Surfaces and Thin Layers* **1997**, 1–4.

[42] C.-H. Ma, J.-H. Huang, H. Chen, *Thin Solid Films* **2002**, *418*, 73–78.

[43] C. Prabhakar, G. B. Reddy, C. M. Reddy, D. Nageshwar, A. S. Devi, J. M. Babu, K. Vyas, M. R. Sarma, G. O. Reddy, *Organic Process Research & Development* **1999**, *3*, 121–125.

[44] B. J. Lister, M. Poland, R. E. DeLapp, *The American Journal of Medicine* **2002**, *95*, S2–S9.

[45] C. P. Price, A. L. Grzesiak, M. Lang, A. J. Matzger, *Crystal Growth & Design* **2002**, *2*, 501–503.

[46] L. J. Chyall, J. M. Tower, D. A. Coates, T. L. Houston, S. L. Childs, *Crystal Growth & Design* **2002**, *2*, 505–510.

[47] C. Reichardt, T. Welton, *Solvents and solvent effects in organic chemistry*, John Wiley & Sons, **2011**.

[48] J. A. Riddick, W. B. Bunger, T. K. Sakano, **1986**.

[49] J.-H. Kim, H.-K. Choi, *International Journal of Pharmaceutics* **2002**, *236*, 81–85.

[50] Farzana Hussain, Mehdi Hojjati, Masami Okamoto, Russell E. Gorga, *Journal of Composite Materials* **2006**, *40*, 1511–1575.

[51] A. Alexandrov, L. Smirnova, N. Yakimovich, N. Sapogova, L. Soustov, A. Kirsanov, N. Bityurin, *Applied Surface Science* **2005**, *248*, 181–184.

[52] K. Hamad, M. Kaseem, F. Deri, *Journal of Materials Science* **2011**, *46*, 3013–3019.

[53] G. Odian, *Principles of polymerization*, John Wiley & Sons, **2004**.

[54] Xi-Wen Du and Ying-Song Fu and Jing Sun and Xue Han and Jim Liu, *Semiconductor Science and Technology* **2006**, *21*, 1202.

[55] J. Nyvlt, *Crystal Research and Technology* **1995**, *30*, 443–449.

[56] A. Levin, T. O. Mason, L. Adler-Abramovich, A. K. Buell, G. Meisl, C. Galvagnion, Y. Bram, S. A. Stratford, C. M. Dobson, T. P. Knowles, *Nature communications* **2014**, *5*, 5219.